ICPMAT-2022

16th International Conference on

Physical Properties and Application of Advanced Materials

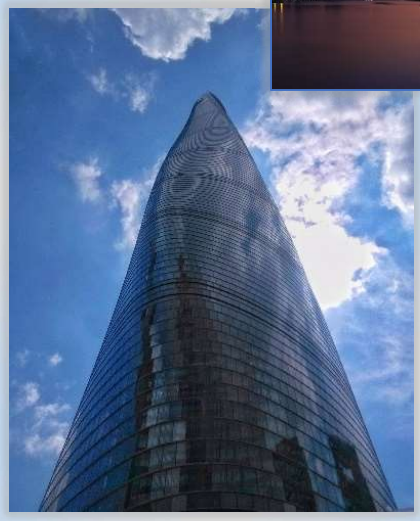

November 21-23, 2022, Shanghai, China

Organized by:

Materials Genome Institute of Shanghai University

Zhejiang Laboratory

Shanghai Physical Sociaty

Shanghai Laue Science and Technology Institute

16th International Conference on the Physical Properties and Application of Advanced Materials (ICPMAT2022)

The International Conference on the Physical Properties and Application of Advanced Materials (ICPMAT) is an annual conference founded by Shanghai University, University of Toyama and Japan Institute of Metals, and is organized by a selected host country. The conference focuses on fundamental and applied researches and current developments in physics and materials science, including raw materials, structural materials, functional materials, advanced characterization techniques and computational materials science. The conference aims to further explore the topics, bring the community closer together, and foster discerning discussions and new collaborations.

ICPMAT2022 will be hosted by Shanghai University and Zhejiang Laboratory, China. The conference will be held as a hybrid event, where local participants will attend in person in the city of Shanghai, and overseas participants are welcome to travel to China, but if not possible, they can choose to attend virtually. More information can be found on the conference website: https://icpmat2022.scievent.com.

■ Conference Topics

- Advanced Functional Materials
- Computational Materials
- Data Driven Materials Design
- Metallurgical Engineering
- Quantum Materials
- Structural Materials

■ Conference Chair

Jun-Yi Ge, *Shanghai University, China*

■ Co-Chairs

Marco Actis Grande, Politecnico di Torino, Italy

Atsushi Saiki, University of Toyama, Japan

■ Organized by

Shanghai University, China

Zhejiang Laboratory, China

■ Co-organized by

University of Toyama, Japan

■ International Committee Member:

Chair: Jincang Zhang, *Shanghai University and Zhejiang Laboratory, China*

Co-chair: Katsuhiko Nishimura, University of Toyama, Japan

Guang-hui Min，Shandong University, China

Marco Actis Grande，*Politecnico di Torino, Italy*
Tetsuo Aida，*University of Toyama, Japan*
Chaiyasit Banjongprase，*Chiang mai University, Thailand*
Jana Bidulska，*Technical University of Kosice, Slovakia*
Shixun Cao，*Shanghai University, China*
Torranin Chairuangsri，*Chiang mai University, Thailand*
Renchao Che，*Fudan University and Zhejiang Laboratory, China*
R. Holmestad，*Norwegian University of Science and Technology, Norway*
Yuukou Horita，*University of Toyama, Japan*
Wayne D. Hutchison，*University of New South Wales, Australia*
Takuya Ishimoto，*University of Toyama, Japan*
Dang Quoc Khanh，*Hanoi University of Science and Technology, Vietnam*
Pham Mai Khanh，*Hanoi University of Science and Technology, Vietnam*
Tibor Kvackaj，*Technical University of Kosice, Slovakia*
Malgorzata Lewandowska，*Warsaw University of Technology, Poland*
Zhe Li, *Harbin Institute of Technology (Shenzhen), China*
Le Van Lich，*Hanoi University of Science and Technology, Vietnam*
Lidia Lityńska Dobrzyńska，*Polish Academy of Sciences, Poland*

Knut Marthinsen, *Norwegian University of Science and Technology, Norway*
Calin D. Marioara, *SINTEF, Norway*
Kenji Matsuda，*University of Toyama, Japan*
Sarka Mikmekova, *Institute of Scientific Instruments of the CAS, v.v.i., Czech Republic*
Ilona Mullerova, *Czech Academy of Sciences, Czech Republic*

Mitsuhiro Murayama，*Virginia Tech, USA*
Katsuhiko Nishimura，*University of Toyama, Japan*
Norio Nunomura，*University of Toyama, Japan*
Hedeki Ono，*University of Toyama, Japan*
Kedsarin Pimraksa，*Chiang mai University, Thailand*
Wei Ren，*Shanghai University, China*
Jincang Zhang，*Shanghai University and Zhejiang Laboratory, China*
Seiji Saikawa，*University of Toyama, Japan*
Atsushi Saiki，*University of Toyama, Japan*
Toshiya Shibayangi，*University of Toyama, Japan*
Gary J. Shiflet，*University of Virginia, USA*
Mirosław Stygar，*AGH University of Science and Technology, Poland*
Yutaka Takaguchi，*University of Toyama, Japan*
Tohru Watanabe，*University of Toyama, Japan*

■ Organizing Committee

Chair：**Guixin Cao**，*Shanghai University, China*

Co-chair：**Kenji Matsuda,** *University of Toyama, Japan*

Yong Zou，*Shandong University, China*

Jie Wang，*Zhejiang Laboratory and Zhejiang University, China*

Members:

Jian Yu, *Donghua University, China*
Sheng Sun, *Shanghai University, China*
Yifeng Cheng, *Zhejiang Laboratory, China*
Zhenjie Feng, *Shanghai University, China*
Fei Chen, *Shanghai University, China*
Jinke Bao, *Shanghai University, China*
Yunhong Zhao, *Zhejiang Laboratory, China*
Rongrong Jia, *Shanghai University, China*
Wenlai Lu, *Shanghai University, China*

General Secretary

Baojuan Kang, *Shanghai University, China*

Scientific Programs

Information for Presenter and Chair

Oral Sessions

All speakers must report to the session chairs prior to the beginning of the session.

The allocation for each oral presentation is 25 minutes.

a) 20 minutes for the presentation

b) 5 minutes for Q&A

Guideline for the Oral Sessions

The Chair of each oral session is expected to enter in the VooV meeting room (each conference number can be found in the program) at least 10 minutes prior to the session.

Due to the impact of COVID-19, the entire meeting will be conducted online. Each oral speaker should open your MS PowerPoint in advance. After the Q&A session of the previous speaker, you should follow the chairman's instruction to share your screen and start the presentation.

Due to the large number of participants this time, the meeting schedule is tight, each speaker should present his/her work in time.

Poster Sessions

There are three parallel poster sessions going on at the same time. All poster speakers must report to the session chairs prior to the beginning of the session.

The allocation for each poster presentation is 7 minutes.

a) 5 minutes for the presentation

b) 2 minutes for Q&A

Guideline for the Poster Sessions

The Chair of each oral session is expected to enter in the VooV meeting room (each conference number can be found in the program) at least 10 minutes prior to the session.

Due to the impact of COVID-19, the entire meeting will be conducted online. Each oral speaker should open your MS PowerPoint in advance. After the Q&A session of the previous speaker, you should follow the chairman's instruction to share your screen and start the presentation.

Due to the large number of participants this time, the meeting schedule is tight, each speaker should present his/her work in time.

Program at a glance

DAY-1: 21 November 2022 (Monday)				
21 November, 2022 14:00-14:25 (Beijing Time) Conference Opening			VooV Conference Number: 952-395-950	Password: 2022
Chairman: Junyi Ge				
Date	Speech by experts and leaders	Reporter	Institution	Title
2022/11/21pm	Opening speech 01 14:00-14:05	Junyi Ge	Shanghai University	Welcome Address
	Opening speech 02 14:05-14:15	Kenji Matsuda	University of Toyama	Openning Speech
	Opening speech 03 14:15-14:25	Yong Zou	Shandong University	Openning Speech
	21 November, 2022 14:25-17:05 (Beijing Time) The conference report			
	Session 1 Chairman: Kenji Matsuda			
	Report number and time	Reporter	Institution	Title
	O1-Oral Talk 14:25-14:50	Wei Ren	Shanghai University	Unconventional ferroelectricity and physical effects in simple binary compounds
	O2-Oral Talk 14:50-15:15	Abrar Ahmed	University of Toyama	TEM observation of Al-Zn-Mg alloy with low Zn/Mg ratio
	O3-Oral Talk 15:15-15:40	Jiong Yang	Shanghai University	High-Throughput Design of Thermoelectrics Based on MatHub-3d Repository and Search of the Key Features
	Coffee Break 15:40-15:50			
	Session 2 Chairman: Marco Actis Grande			
	Report number and time	Reporter	Institution	Title
	O4-Oral Talk 15:50-16:15	Miroslaw Stygar	AGH University of Science and Technology	The structures and properties of functional high-entropy spinel materials
	O5-Oral Talk 16:15-16:40	Vladimir Gladilin	Antewerp University	Vortices in lattices of nonequilibrium photon condensates
	O6-Oral Talk 16:40-17:05	Knut Marthinsen	Norwegian University of Science and Technology	Orientation dependent Zener-pinning of sub-grains during recovery and recrystallization of an Al-Mn alloy
DAY-2: 22 November 2022 (Tuesday)				
22 November, 2022 08:30-17:00 (Beijing Time) The conference report			VooV Conference Number: 592-633-959	Password: 2022
Session 1 Chairman: Yong Zou				
Date	Report number and time	Reporter	Institution	Title
2022/11/22am	O7-Oral Talk 08:30-08:55	Zhenjie Feng	Shanghai University	Development of Laboratory Atomic Pair Distribution Function X-ray diffractometer
	O8-Oral Talk 08:55-09:20	Yu Gao	Shandong University	Machine learning accelerated design of non-equiatomic Refractory High Entropy Alloys based on First principles calculation
	O9-Oral Talk 09:20-09:45	Yalei Huang	Shanghai University	Anomalous resistivity upturn in the van der Waals ferromagnet Fe_5GeTe_2
	O10-Oral Talk 09:45-10:10	Hiroki Saito	University of Toyama	Effect of total amount of Cu, Mg and cold rolling on age precipitation of Al-Cu-Mg alloys
	Coffee Break 10:10-10:20			
	Session 2 Chairman: Shixun Cao			
	Report number and time	Reporter	Institution	Title
	O11-Oral Talk 10:20-10:45	Haruki Tsukuda	University of Toyama	Microstructural observation of Al-based TiAl composites fabricated by 3DPC
	O12-Oral Talk 10:45-11:10	Xiaoxuan Ma	Shanghai University	Tuning spin reorientation transition and spin switching in praseodymium-erbium orthoferrites single crystals
	O13-Oral Talk 11:10-11:35	Auekarn Chuwongwittaya	Chiang Mai University	Geopolymer/Zeolite P Composites from Combustion By-products
Lunch Break 11:35-13:00				
Session 3 Chairman: Shenghao Wang				
Date	Report number and time	Reporter	Institution	Title
2022/11/22pm	O14-Oral Talk 13:00-13:25	Xinyu Yao	Shanghai University	Orbital two-channel Kondo effect in antiferromagnetic Weyl semimetal Mn_3Ge
	O15-Oral Talk 13:25-13:50	Norikazu Jinno	University of Toyama	Effect of Sn on Segregation Behavior of Si during Solidification of Molten Steel
	O16-Oral Talk 13:50-14:15	Wanting Yang	Shanghai University	The spin-switching and magnetocaloric research in Tb doped $YbFeO_3$ single crystal
	O17-Oral Talk 14:15-14:40	Jinke Bao	Shanghai University	Spin and charge density waves in the quasi-one-dimensional KMn_6Bi_5
	O18-Oral Talk 14:40-15:05	Chang Liu	Shandong University	Effect of Nb content on the microstructure and corrosion resistance of $FeCoCrNiNb_x$ high entropy alloy in chloride ion environment
	Coffee Break 15:05-15:15			
	Parallel Poster Session 1 Chairmen: Guixin Cao, Fei Chen		VooV Conference Number: 592-633-959	Password: 2022
	Report number and time	Reporter	Institution	Title
	P1-Poster 15:15-15:22	Keisuke Maida	University of Toyama	Effect of Injection Molding Conditions on Dimensional Accuracy and Mechanical Properties of Carbon Fiber Reinforced PEEK
	P2-Poster 15:22-15:29	Yanhong Chen	Shanghai University	Organic Lead-based Halide Perovskite Single Crystal for High-performance Photodetector
	P3-Poster 15:29-15:36	Shun Kawamata	University of Toyama	Microstructure evolution of Al-1.0Mg-0.6Si(mass%) alloys with homogenization treatment
	P4-Poster 15:36-15:43	Huan Song	Shanghai University	Spin switch effect of TmFeO3 under low magnetic field
	P5-Poster 15:43-15:50	Masahiro Yamagami	University of Toyama	Hot electron extraction in SWCNT/TiO2 for photocatalytic H2 evolution from water
	P6-Poster 15:50-15:57	Zhigiang Sun	Shanghai University	Spin switching effect in Nd0.8Pr0.2FeO3 single crystal
	P7-Poster 15:57-16:04	Naru Akiyama	University of Toyama	Evaluation of electrochemical properties of batteries prepared by aerosol deposition method
	P8-Poster 16:04-16:11	Shuang Zhu	Shanghai University	Magnetodielectric effect and magnetoelectric coupling of $Co_2NiNb_2O_8$ single crystal
	P9-Poster 16:11-16:18	Shotaro Kawara	University of Toyama	Growth of lithium niobate single crystals using the floating zone method and changes in physical properties due to Na addition
	P10-Poster 16:18-16:25	Lixin Cao	Shanghai University	Flux Pinning Evolution of Pb Multilayer Thin Films in the purely repulsive interaction system
	P11-Poster 16:25-16:32	Yusuke Sekiguchi	University of Toyama	Mechanical properties and precipitation of Al-4mol%Zn-2mol%Mg-1mol%Cu alloy
	P12-Poster 16:32-16:39	Weibin Wu	Shanghai University	Crystal growth and physical properties evolution in Ni1-xCoxTe2-δ system
	P13-Poster 16:39-16:46	Sumitaka Yamaguchi	University of Toyama	Superconductive Property of Nb3Al/Al Composite Materials
	P14-Poster 16:46-16:53	Jingyu He	Shanghai University	The effect of granularity on superconducting properties of Pb films
	P15-Poster 16:53-17:00	Shoya Ukita	University of Toyama	DSC analysis and TEM microstructure observation of Al-1.0Mg2Ge alloy
	Parallel Poster Session 2 Chairmen: Knut Marthinsen, Jinke Bao		VooV Conference Number: 602-454-611	Password: 2022
	Report number and time	Reporter	Institution	Title
	P16-Poster 15:15-15:22	Tomoki Miyazono	University of Toyama	Yttrium and Praseodymium doped proton conducting electrolytes with improved sinterability
	P17-Poster 15:22-15:29	Jiafeng Chen	Shanghai University	Superconducting state properties of Cu-doped $NbTe_2$ single crystals
	P18-Poster 15:29-15:36	Kodai Yabashi	University of Toyama	Effect of injection molding conditions of carbon fiber reinforced PEKEKK resin on retainer
	P19-Poster 15:36-15:43	Yifeng Zhang	Shanghai University	Microstructure and microwave absorption properties of FeCoNiCuGe high-entropy alloys
	P20-Poster 15:43-15:50	Yuichi Kirimoto	University of Toyama	Investigation of manufacturing conditions of single roll rapidly solidified ribbon for anode materials of Mg rechargeable batteries by using thermal-hydraulics CAE
	P21-Poster 15:50-15:57	Weihao Shen	Shanghai University	Magnetic phase transitions and giant magnetic coercivity in Mn2.45Fe0.58Sn0.97 single crystals
	P22-Poster 15:57-16:04	Kosuke Fuke	University of Toyama	Effect of process parameters on anode activity of Mg-6%Al-3%Ca alloy ribbons manufactured by single-roll atmospheric rapid solidification method for Mg rechargeable batteries
	P23-Poster 16:04-16:11	Guang Wu	Shanghai University	High-throughput X-ray characterization of discrete component samples of rare earth-doped thermal barrier coating materials
	P24-Poster 16:11-16:18	Ginji Ota	University of Toyama	Effect of Ag Addition on Corrosion Properties of Mg-Al Alloys
	P25-Poster 16:18-16:25	Yuzhe Pan	Shandong University	Stress corrosion behavior of friction stir welding joint of 7N01 aluminum alloy
	P26-Poster 16:25-16:32	Tomohiro Fujimoto	University of Toyama	B substitution effect on magnetic properties of HoAl2
	P27-Poster 16:32-16:39	Shuting Yu	Shanghai University	Optimization of the mechanical properties of SAC105-based solder alloys via machine learning
	P28-Poster 16:39-16:46	Nguyen Khanh Huyen	University of Toyama	$MoSe_2$-sensitized water splitting assisted by C60-dendron on the basal surface
	P29-Poster 16:46-16:53	Erika Ilida	University of Toyama	Magnetic properties of Al-4%Cu(-Mn, -Fe) alloy
	P30-Poster 16:53-17:00	Syoma Yoshinaga	University of Toyama	Magnetocaloric properties of Ho1-xGdxB2
	Parallel Poster Session 3 Chairmen: Zhenjie Feng, Rongrong Jia		VooV Conference Number: 292-880-529	Password: 2022
	Report number and time	Reporter	Institution	Title
	P31-Poster 15:15-15:22	Chuanyi Wu	Shanghai University	Superconductivity of La (111)/Si (100) thin films
	P32-Poster 15:22-15:29	Yuto Arata	University of Toyama	Effect of rare earth addition on sodium tantalate prepared by solution process
	P33-Poster 15:29-15:36	Tianyuan Li	Shanghai University	Effect of alloying elements on the microstructure and properties of SnAgCu based lead-free solder alloys
	P34-Poster 15:36-15:43	Shuhei Murakata	University of Toyama	Microstructure observation of Al-1.0mass%Mg2Ge-(0.4mass%Si) alloys aged at 473K
	P35-Poster 15:43-15:50	Jiajie Zhang	Shanghai University	Long-range ferromagnetic ordering and novel phase transitions in macroscopic artificial kagome particle ice
	P36-Poster 15:50-15:57	Jun Ezura	University of Toyama	TEM observation of Mg-2.2Zn-0.2In alloy aged at 473K
	P37-Poster 15:57-16:04	Luman Hou	Shanghai University	Reveal of free radicals in manganese-based catalysts and their roles during selective catalytic reduction of nitrogen oxide
	P38-Poster 16:04-16:11	Takashi Hashizume	University of Toyama	Synthesis of micro sized hollow Ceria particles prepared by spray dry pyrolysis
	P39-Poster 16:11-16:18	Daichi Nakato	University of Toyama	Effect of Mo on Pitting Corrosion Resistance of Martensitic Stainless Steels
	P40-Poster 16:18-16:25	Yota Yamada	University of Toyama	Effect of Cu content on electrochemical activity in Mg-Cu binary alloys prepared by single role rapid solidification method
	P41-Poster 16:25-16:32	Yangzhou Wang	Shanghai University	High-throughout synthesis of La1-xSrxTiO3 thin film and its characterizations
	P42-Poster 16:32-16:39	Hideki Minami	University of Toyama	Effect of microstructure on hardness of Mg-Sc-Zr alloys with α + β dual phase

DAY3: 23 November 2022 (Wednesday)				
23 November, 2022 09:00-16:50 (Beijing Time) The conference report			VooV Conference Number: 345-240-020	Password: 2022
Session 1 Chairman: Jiong Yang				
Date	Report number and time	Reporter	Institution	Title
2022/11/23am	O19-Oral Talk 09:00-09:25	Kai Chong	Shandong University	Thermal stability and corrosion behavior of a novel $Zr_{22.5}Ti_{22.5}Hf_{22.5}Ni_{22.5}Ta_{10}$ high-entropy amorphous alloy
	O20-Oral Talk 09:25-09:50	Chenfei Shi	Shanghai University	The microstructure and magnetic properties of Fe ion doped $GdCrO_3$
	O21-Oral Talk 09:50-10:15	Atsushi Saiki	University of Toyama	Surface modification of aluminum alloy by local laser irradiation
	O22-Oral Talk 10:15-10:40	Tian He	Shanghai University	Flux pinning behavior and related physical mechanism of $CaKFe_4As_4$ superconductor
	O23-Oral Talk 10:40-11:05	V. N. Hai	University of Toyama	Effect of thermal aging on the properties and microstructure of Al-Cu-Mg-Si alloy
Lunch Break 11:05-12:30				
Session 2 Chairman: Junyi Ge				
Date	Report number and time	Reporter	Institution	Title
2022/11/23pm	O24-Oral Talk 12:30-12:55	Anlei Zhang	Shanghai University	Electric transport properties of ZrB_{12} micro-bridge
	O25-Oral Talk 12:55-13:20	Yuito Koishikawa	University of Toyama	Data-driven techniques for high-hardness Al-Mg_2Si series alloy to obtain optimal chemical composition
	O26-Oral Talk 13:20-13:45	Jiaying Zhang	Shanghai University	Phase diagram for Fe_3SexTe_{1-x} superconductors
	O27-Oral Talk 13:45-14:10	Ting Xue	Shandong University	Thermophysical and mechanical properties of Al2O3-doped YTaO4 ceramic as potential thermal barrier coating
	O28-Oral Talk 14:10-14:35	Shenghao Wang	Shanghai University	Interfacial and opto-electronic properties of halide perovskites: from toxic to eco-friendly
Coffee Break 14:35-14:45				
Session 3 Chairman: Wei Ren				
	Report number and time	Reporter	Institution	Title
	O29-Oral Talk 14:45-15:10	Guixin Cao	Shanghai University	Field-driven surface state and topological nodal lines in layered semimetals
	O30-Oral Talk 15:10-15:35	Tadayoshi Tsukeda	University of Toyama	Improvement on electrochemical activity of anode materials for magnesium rechargeable batteries by laser processing
	O31-Oral Talk 15:35-16:00	Fei Chen	Shanghai University	Electronic structure of FeS superconductor
	O32-Oral Talk 16:00-16:25	Jiasen Han	Shandong University	Improving CMAS-corrosion resistance of YSZ-based thermal barrier coatings with Al_2O_3 addition
	O33-Oral Talk 16:25-16:50	Mingqian Zhang	Shanghai University	In-situ conversion of amorphous carbon to graphene enhances the oxidation resistance of dendritic copper powder
23 November, 2022 16:50-17:10 (Beijing Time) Conference Closing				
Chairman: Junyi Ge				
Date	Speech by experts and leaders	Reporter	Institution	Title
2022/11/23pm	Closing speech 01 16:50-17:00	Junyi Ge	Shanghai University	Closing Address
	Closing speech 02 17:00-17:10	Marco Actis Grande	Politecnico di Torino	Closing Speech

Abstract Book

O1- Unconventional ferroelectricity and physical effects in simple binary compounds

W. Ren

Department of Physics, Shanghai University 200444, Shanghai, China.

First-principles calculations are performed to investigate ferroelectricity in some binary compounds, including bilayer two-dimensional (2D) hexagonal boron nitride (h-BN) and rocksalt oxide family (AO with A=Cd, Ba, Sr, Ca, Mg, etc.) via the application of biaxial strain. The origins of such unconventional ferroelectricity are discussed from the lattice perspective and electronic structure properties. These findings have the potential to motivate the study of simple materials possessing ferroelectricity and piezoelectricity that may lead to novel devices.

Email: renwei@shu.edu.cn

ICPMAT 2022 Shanghai 中国
16th International Conference on the Physical Properties and Application of Advanced Materials
21st-23rd November, 2022

O2-TEM observation of Al-Zn-Mg alloy with low Zn/Mg ratio

A. Ahmed[1‡], S. Lee[2], T.Tsuchiya[2], Kenji Matsuda[2†], K. Nishimura[2], N. Nunomura[2], H. Toda[3], K. Hirayama[4], K. Shimizu[5], M. Yamaguchi[6], T. Tsuru[6], M. Itakura[6]

1 *Graduate School of Science and Engineering, University of Toyama, Toyama, Toyama, 930-8555, Japan*

2 *Faculty of Sustainable Design, University of Toyama , Toyama, Toyama, 930-8555, Japan*

3 *Department of Mechanical Engineering, Kyushu University, Fukuoka, 819-0395, Japan*

4 *Department of Materials Science and Engineering, Kyoto University, Kyoto, 606-8501, Japan*

5 *Department of Physical Science and Materials Engineering, Iwate University, Iwate, 020-8551, Japan*

6 *Nuclear Science and Engineering Center, Japan Atomic Energy Agency, Ibaraki, 319-1195, Japan*

The influence of the Zn/Mg ratio on the microstructure and mechanical properties of Al-Zn-Mg alloys with a low Zn/Mg ratio has been investigated through microhardness tests and transmission electron microscopy (TEM). Due to their excellent mechanical qualities and formability, Al-Zn-Mg alloys have been widely used in structural load-bearing components of the automotive and aerospace industries. Precipitation strengthening was the primary strengthening mechanism, similar to other heat-treatable alloys. Al-Zn-Mg alloys must be developed with both the overall Zn and Mg contents and the Zn/Mg ratio in thought to work at their best. According to various researchers, the major strengthening phase occurred after peak ageing when the Zn/Mg ratio was between 2 and 3, and the T phase when the ageing temperature was over 200°C. Due to the excellent strengthening effect of the η′ phase, extensive research has been done on its precipitation sequence, composition, atomic structure, and phase transformation mechanism for many years. In contrast, the T′ phase of Al-Zn-Mg alloys, which has a weakening effect, has received much less attention. T phase has a body-centered cubic structure, a=1.416 nm for the lattice parameter, and $Mg_{32}(Al, Zn)_{49}$ or $Mg_3Zn_3Al_2$ for the stoichiometry. The most significant precipitates were considered to be the $MgZn_2$ phase (η phase) and its metastable phase (η′ phase). In Al-Zn-Mg alloys with low Zn and high Mg content, other research also discovered that there were several $Mg_{32}(Al, Zn)_{49}$ phase (T phase) and its metastable phase (T′ phase). For this study, I decided to use Al-Zn-Mg alloys with a Zn/Mg ratio of 0.71. According to the observations, the alloy with a Zn/Mg ratio of 0.71 aged at 200 °C for 2000 minutes had the maximum Vickers hardness. According to TEM observations, the examined alloy's strengthening precipitates were usually T′ or T phase.

Keywords: Microstructure structure, Microhardness, Precipitation.

Email: †ikenolab@sus.u-toyama.ac.jp

O3 - High-Throughput Design of Thermoelectrics Based on MatHub-3d Repository and Search of the Key Features

J. Yang[1,2*]

[1]*Materials Genome Institute, Shanghai University, Shanghai, 200444, China;*

[2]*Zhejiang Laboratory, Hangzhou, Zhejiang 311100, China*

Since 2011, there have been emerging several computational material databases, including the Materials Project, AFLOW, Atomly, and MatHub-3d(2d) from MGI, Shanghai University. MatHub-3d aims at the electrical and thermal transport properties; the repository contains over 80,000 inorganic structures, over 30,000 electronic structures, and over 10k electrical transport properties.[1] This talk will cover several recent high-throughput screening works for new thermoelectrics based on the MatHub-3d. In the search of new thermoelectrics, besides the screening from direct calculations of transport properties, the search can also be accelerated by the key features. Based on the previous study that the carrier type of semiconductors relate to the band edge energy position, we propose the strategy of searching n-type Cu-contained compounds by looking for compounds with low-energy conduction band minima. Follow-up theoretical and experimental studies confirm this strategy, and obtain a new thermoelectric compound CuIn5Se8 with experimentally ZT of 0.84.[2] In another study, we propose a new concept of "Functional-unit design", borrowed from the "fragment design" in the search of new drug. A linear triatomic bonding is found to be an effective thermoelectric functional unit. This unit is theoretically proved to cause large lattice anharmonicity and band anisotropy, both favoring the thermoelectric performance. The predicted compound K5CuSb2 has a ZT value of 1.3.[3] The two case studies demonstrate the powerfulness of the combination of material repository and key feature search in accelerating the high-throughput works.

Keywords: MatHub-3d; Key feature; Energy position; Functional-unit design

Email: jiongy@t.shu.edu.cn

ICPMAT 2022 Shanghai 中国
16th International Conference on the Physical Properties and Application of Advanced Materials
21st-23rd November, 2022

O4- The structures and properties of functional high-entropy spinel materials

Mirosław Stygar[1]‡, J. Dąbrowa[1], M. Zajusz[1], E. Durda[1], M. Moździerz[2], K. Matsuda[3]

[1]*AGH University of Science and Technology, Faculty of Materials Science and Ceramics, Kraków, Poland*

[2]*AGH University of Science and Technology, Faculty of Energy and Fuels, Kraków, Poland*

[2]*University of Toyama, Faculty of Sustainable Design, Toyama, Japan*

The synthesis, structure, and properties of the high-entropy spinels are discussed on the example of compositions from the Co-Cr-Fe-Mg-Mn-Ni-O system. The single-phase $(Co,Cr,Fe,Mn,Ni)_3O_4$, $(Cr,Fe,Mg,Mn,Ni)_3O_4$, and $(Co,Cr,Fe,Mg,Mn)_3O_4$ materials are obtained, together with the selected quaternary subsystems. The stability of the materials, both in terms of the temperature and oxygen partial pressure dependence is evaluated, showing the profound influence of these parameters on the spinel-forming capabilities of the investigated systems, potentially providing means for further tailoring of their structure, including the transition between *Fd*-3*m* spinel symmetry and *Fm*-3*m* rocksalt one. Thermomechanical behavior of all single-phase compositions is remarkably similar, with the values of thermal expansion coefficient being in the range of 8.8 to 9.8·10 K^{-1}, making the materials potentially interesting in terms of compatibility with materials used in the solid oxide fuel cell technology (SOFC), especially interconnects. The temperature dependence of the electrical conductivity indicates the semiconducting character, with a clearly visible change of the energy activation *ca.* 400 °C. To provide a further understanding of these systems, the initial assessment of the cationic occupancy within the tetra- and octahedral lattice sites is carried out for selected compositions, through the use of the Mossbauer spectroscopy measurements combined with the density functional theory *ab initio* calculations (DFT).

The results show distinctively different tendencies between quaternary subsystems and $(Co,Cr,Fe,Mn,Ni)_3O_4$ composition. In the case of the former ones, a preferential occupancy of the lattice sites appears to be energetically favourable, while for the quinary composition, the entropic configuration on both sublattices turns out to be characterized by the lowest energy. The potential for tailoring the occupancy of cationic lattice sites by the introduction of the specific cations is discussed.

Based on the analogy to conventional spinels, as well as the determined electrical and thermomechanical properties of the studied high-entropy spinels, their application as protective-conductive coatings for interconnect elements in SOFCs is proposed. Taking into account some of the established features of the high-entropy systems, such as lattice distortion, potentially affecting the rate of cations' diffusion, it can be postulated that they may carry significant potential with regard to this technology, especially in terms of corrosion protection and suppression of the deleterious Cr-poisoning effect. The initial studies regarding the possibility of applying such coatings on the Crofer 22APU ferritic stainless steel substrate are carried out, together with the preliminary performance assessment of the obtained ceramic/metallic system.

Keywords: High entropy oxide, Spinel structure, Solid Oxide Fuel Cell, Interconnects, Conductive coating

Email: ‡stygar@agh.edu.pl

O5-Vortices in lattices of nonequilibrium photon condensates

Vladimir N. Gladilin‡ and Michiel Wouters
TQC, Universiteit Antwerpen, Universiteitsplein 1, B-2610 Antwerpen, Belgium

The creation of photonic Bose-Einstein condensates (BECs), formed due to thermalization of cavity photons through repeated absorption and emission by dye molecules, has presented an invitation to study these systems from a quantum fluid perspective. For superfluids, vortex excitations play a crucial role in a variety of phenomena such as the Berezinskii–Kosterlitz–Thouless (BKT) transition, Kibble–Zurek scenario, formation of vortex lattices, and the drag force on objects moving through a superfluid. Here we present the results of our theoretical study of vortices in arrays of photon condensates. Because of cavity mirror losses, optical BECs need constant pumping by an excitation laser in order to reach a steady state and experimentally realized photon condensates are therefore driven-dissipative systems. We show that, even when interactions are negligible, as is the case in current experiments on photonic BECs, pumping and losses can lead to a finite vortex core size. While some properties of photon-condensate vortices, such as their self-acceleration, the formation of outward particle flows from the vortex cores, and the generation of vortex pairs by a moving vortex resemble those in lasers and interacting exciton-polariton condensates far from equilibrium, in several aspects they differ from previously studied systems: the vortex core size is determined by the balance between pumping and tunneling, the core appears oblate in the direction of its motion, and new baby-vortex pairs can spontaneously nucleate in the core region. We also demonstrate that, due to outward currents from the vortex cores, in combination with quasicircular motion of self-accelerated vortices, a repulsive gas of low-mobility vortices and antivortices can be formed, where the pair annihilation is dramatically slowed down. At the same time, our numerical and analytical investigations of the BKT transition in a lattice condensate of noninteracting photons show that the vortex-free phase is actually stabilized by driving and dissipation.

Keywords: Nonequilibrium systems, Bose-Einstein condensates, Cavity resonators, Vortices in superfluids
Email: ‡vladimir.gladilin@uantwerpen.be

ICPMAT 2022 Shanghai 中国
16th International Conference on the Physical Properties and Application of Advanced Materials
21st-23rd November, 2022

O6-Orientation dependent Zener-pinning of sub-grains during recovery and recrystallization of an Al-Mn alloy

Håkon W Ånes[1], Antonius T.J. van Helvoort[2], Knut Marthinsen[1], ‡

[1]*Department of Materials Science and Engineering, Norwegian University of Science and Technology (NTNU), N-7491 Trondheim, Norway.*

[2]*Department of Physics, Norwegian University of Science and Technology (NTNU)), N-7491 Trondheim, Norway*

Correlated analysis of (sub)grains and particles in alloys is important to understand transformation processes and control material properties. A multimodal data fusion workflow directly combining subgrain data from electron backscatter diffraction (EBSD) and particle data from backscatter electron (BSE) images in the scanning electron microscope has therefore been developed. Correlated analysis of secondary phase particles down to 0.03 μm in diameter and subgrains and subgrain boundaries is enabled by the higher fidelity of the BSE images. The workflow is demonstrated on a cold-rolled and recovered Al-Mn alloy, where constituent particles formed during casting and dispersoids formed during subsequent heating affect recovery and recrystallization upon annealing. The multimodal dataset enables statistical analysis including subgrains surrounding constituent particles and dispersoids' location with respect to subgrain boundaries. Counting dispersoids at subgrain boundaries shows a lower Smith-Zener drag for P-oriented subgrains ({011}<122>) (and to some extent also ND-rotated Cube) as compared to other typical recrystallization components, notably Cube, thus bringing clues to the strong P-texture often observed in AlMn alloys in conditions of strong concurrent precipitation.

Keywords: Al-Mn alloy, Recovery and recrystallization, Correlated SEM BSE/SEM-EBSD analysis, Dispersoid-subgrain boundary correlations, Zener pinning

Email: ‡knut.marthinsen @ntnu.no

ICPMAT 2022 Shanghai 中国
16th International Conference on the Physical Properties and Application of Advanced Materials
21st-23rd November, 2022

O7-Development of Laboratory Atomic Pair Distribution Function X-ray diffractometer

Z. J. Feng [1,2,3,4*]

[1]*Materials Genome Institute, Shanghai University, Shanghai, 200444, China*
[2]*Zhejiang Laboratory, Hangzhou 311100, China*
[3]*Shanghai Laue Sci. & Tech. Institute, Shanghai, 2*00444, China
[4]*Shanghai Key Laboratory of High Temperature Superconductors, Department of Physics, Shanghai University, Shanghai, 200444, China*

In recent years, with the rapid development of science and technology, the application field of diffractometer is expanding rapidly. The demand for the high performant diffractometer is higher and higher, so it is necessary to develop more advanced diffractometer. On the other hand, the technology of the core key components of domestic X-ray diffractometer has made great progress, which provides a hardware basis for the research and development of domestic high-performance X-ray diffractometer. The superposition of these two factors provides an opportunity for us to develop domestic high-performance X-ray diffractometer. This lecture mainly introduces the development of domestic key components and domestic high-performance fast X-ray diffractometer to meet the needs of in-situ fast X-ray diffractometer, material genome engineering high-flux diffractometer and atomic distribution function analysis technology.

Keywords: Materials Genome Initiative; High throughput; atomic pair distribution function; PDF
Email: fengzhenjie@shu.edu.cn

O8-Machine learning accelerated design of non-equiatomic Refractory High Entropy Alloys based on First principles calculation

Y. Gao[1], Y. Zou[*2]

[1]*School of Materials Science and Engineering, Shandong University, Jinan, Shandong, 250061, China*

[2]*Shandong Engineering & Technology Research Center for Modern Welding, Shandong University, Jinan, Shandong, 250061, China*

The properties of High Entropy Alloys (HEAs) strongly depend on the composition and content of elements. However, it was difficult to obtain the optimized element composition through the traditional "trial and error" method. The non-equiatomic HEAs have a large range for composition exploration by changing the content of elements, but the current research methods are difficult to analyze comprehensively. In this work, the prediction model with high accuracy is established by mixture design, the first principles calculation and machine learning. The model is used to predict the elastic properties and Poisson's ratio of non-equiatomic Mo-Nb-Ta-Ti-V HEAs, and the prediction results agree well with experimental data. The optimal element composition range of elastic properties and Poisson's ratio could be obtained. The influence of elements on the elastic properties and Poisson's ratio is analyzed through the calculation of features' importance. The results show that the content of Ti has the greatest contribution to the elastic properties and Poisson's ratio of the alloy. This model can not only obtain a large amount of data quickly and accurately but also help us to establish the relationship between element content and mechanical properties of non-equiatomic Mo-Nb-Ta-Ti-V RHEAs and provide theoretical guidance for experiments.

Keywords: Non-equiatomic refractory high entropy alloys; The first-principles calculation; Machine learning; Elastic properties

Email: yugao08@outlook.com

O9-Anomalous resistivity upturn in the van der Waals ferromagnet Fe_5GeTe_2

Y. L. Huang[1], X. Y. Yao[1], F. Y. Qi[1], W. H. Shen[1], G. X. Cao[1, 2, ‡]

[1]*Materials Genome Institute, Shanghai University, 200444 Shanghai, China*

[2]*Zhejiang Laboratory, Hangzhou 311100, China*

Fe_nGeTe_2 (n = 3, 4, 5) have recently attracted increasing attention due to their two-dimensional van der Waals characteristic and high temperature ferromagnetism, which make promises for spintronic devices. The Fe(1) split site is an important structural characteristic of Fe_5GeTe_2 which makes it very different from other Fe_nGeTe_2 (n = 3, 4) systems. The local atomic disorder and short-range order can be induced by the split site. In this work, the high-quality van der Waals ferromagnet Fe_5GeTe_2 single crystals were grown to study the low-temperature transport properties. We found a resistivity upturn below 10 K. The temperature and magnetic field dependence of the resistivity are in good agreement with a combination of the theory of disorder-enhanced three-dimensional electron–electron and single-channel Kondo effect. The Kondo effect exists only at low magnetic field $B < 3\,T$, while electron-electron dominates the appearance for the low-temperature resistivity upturn. We believe that the enhanced three-dimensional electron–electron interaction in this system is induced by the local atomic structural disorder due to the split site of Fe(1). Our results indicate that the split site of Fe plays an important role for the exceptional transport properties.

Keywords: Fe_5GeTe_2, Electron-electron interaction, Kondo effect

Email: ‡guixincao@shu.edu.cn

ICPMAT 2022 Shanghai 中国
16th International Conference on the Physical Properties and Application of Advanced Materials
21st-23rd November, 2022

O10-Effect of total amount of Cu, Mg and cold rolling on age precipitation of Al-Cu-Mg alloys

H. Saito[1], V. N. Hai[1], T. Tsuchiya[2], S. Lee[2], S. Ikeno[3], and K. Matsuda[2, †]

[1]*Graduate School of Science and Engineering, University of Toyama, Toyama, 930-8555, Toyama, Japan*

[2] *Faculty of Sustainable Design, Department of Materials Design and Engineering, University of Toyama , Toyama, 930-8555, Toyama, Japan*

[3]*Professor emeritus, University of Toyama, Toyama, Japan*

Al-Cu-Mg alloy are cold rolled as 2xxx series aluminum alloys, have been studied to improve and enhance their mechanical properties by using controlling microstructures. Due to its excellent thermal stability and high strength, it is widely used as a high-strength aluminum for the aerospace industry and structures. The aging precipitation process of the Al-Cu-Mg alloy is as follows: supersaturated solid solution→ G.P. zone→ θ' phase→ θ phase ,or supersaturated solid solution→ G.P.B. zone→ S' phase→ S phase depends on their chemical compositions and heat treatment conditions. It is reported that Al-Cu-Mg alloys precipitate Ω phase (Al2Cu) with θ' phase (Al2Cu) and S' phase (Al2CuMg). Many of reports are available that the mechanical properties to of 2xxx series aluminum alloys are improved by thermomechanical treatment, and Ω phase also contributes to increase mechanical properties. Therefore, in this study, Al-Cu-Mg alloy which has Cu/Mg=3, was subjected to four types of cold rolling of 0%, 10%, 30% and 60% before artificial aging to understand how the Cu/Mg ratio to the precipitation of the Ω phase. To investigate mechanical property Vickers microhardness measurement was conducted and TEM observation were performed to observe microstructure. It was confirmed that the maximum hardness was increased with increase of rolling reduction ratio and concentration of Cu and Mg. With TEM observations, the number density of precipitates increased with increasing Cu and Mg. concentration and rolling reduction ratio.

Keyword: Al-Cu-Mg, Precipitate, TEM, Ω phase, Cold-rolling

Email: †ikenolab@sus.u-toyama.ac.jp

ICPMAT 2022 Shanghai 中国
16th International Conference on the Physical Properties and Application of Advanced Materials
21st-23rd November, 2022

O11-Microstructural observation of Al-based TiAl composites fabricated by 3DPC

H. Tsukuda[1], T. Tsuchiya[2], S. Lee[2], S. Ikeno[3], and K. Matsuda[2, †], M. H. Park[4], M. Murayama[5]

[1]Graduate School of Science and Engineering, University of Toyama, Toyama, Toyama, 930-8555, Japan

[2] Faculty of Sustainable Design, Department of Materials Design and Engineering, University of Toyama , Toyama, Toyama, 930-8555, Japan

[3]Professor emeritus, University of Toyama, Toyama, Japan

[4]Graduate School of Engineering, Kyoto University,Kyoto , Kyoto, 606-8501, Japan

[5]Institute for Materials Chemistry and Engineering, Kyushu University, Kasuga, Fukuoka, 816-8580, Japan

The intermetallic compound TiAl is used in the automotive and aerospace industries for turbochargers and jet engines because of its low specific gravity and high-temperature strength . In addition, the regular lattice does not collapse until near the melting point, and since it contains about 30% covalent bonds, the deformation stress shows inverse temperature dependence in the high-temperature region, and it has excellent oxidation resistance and corrosion resistance. Because of these characteristics, TiAl is being put to practical use in various fields. However, TiAl-based intermetallic compounds have some problems, such as poor workability and difficulty in forming without special methods3). 3) In order to solve this problem, we can expect to create a composite material with good workability that has the excellent properties of TiAl by using aluminum, a metallic material with excellent workability and corrosion resistance, as the matrix phase and combining it with particles of intermetallic compound TiAl to create a composite material with good workability.

In TiAl/Al-based composites, there is concern about the formation of coarsened intermetallic compound Al_3Ti when casting is performed; from the equilibrium state diagram of the Al-Ti binary system. We thought that the formation of Al_3Ti could be prevented by casting at a lower molten metal temperature. In this study, we investigated the microstructure and composite properties of the fabricated composites by casting with Al-10%Si alloy, which has a lower melting point than Al, and TiAl particles made of high-purity chemistry.

Keywords: TiAl, Al_3Ti, Composite materials

Email: †ikenolab@sus.u-toyama.ac.jp

O12-Tuning spin reorientation transition and spin switching in praseodymium-erbium orthoferrites single crystals

X. X. Ma[1], N. Yuan[2], W. T. Yang[1], S. Zhu[1], C. F. Shi[1], H. Song[1], Z. Q. Sun[1], B. J. Kang[1], W. Ren[1, 3], S. X. Cao[1, 3‡]

[1]*Department of Physics, Materials Genome Institute and International Center for Quantum and Molecular Structures, Shanghai University, Shanghai 200444, China*

[2]*Kirchhoff Institute of Physics, Heidelberg University, INF 227, D-69120 Heidelberg, Germany*

[3]*Shanghai Key Laboratory of High Temperature Superconductors, Shanghai University, Shanghai 200444, China*

We prepared a series of high-quality single crystal samples of PrxEr1-xFeO3 (x=0, 0.1, 0.3, 0.5) using the optical floating zone method. The crystal structure, quality, and single crystal axis orientation were determined by room temperature powder X-ray diffraction, back-reflection Laue X-ray diffraction, and Raman scattering at room temperature. Magnetic measurements indicate that the spin reorientation transition type and the temperature region of spin reorientation transition can be tuned by introducing different ratios of Pr3+. The trigger temperature of spin switching and magnetization compensation temperature of PrxEr1-xFeO3 crystals can be adjusted by doping with different proportions of Pr3+. Furthermore, the trigger temperature of two types of spin switching of Pr0.3Er0.7FeO3 along a-axis also can be regulated by adjusting the external field. Meanwhile, the magnetic field-triggered spin switching effect can also be observed along the a-axis and c-axis of Pr0.3Er0.7FeO3. An in-depth understanding of the magnetic coupling and competition between the two magnetic sublattices, rare-earth ions sublattice and iron ions sublattice, within the RFeO3 system has important implications for advancing the practical applications of the relevant spin switching materials.

Keywords: Rare-earth orthoferrite, Spin reorientation transition, Spin switching

Email: ‡sxcao@shu.edu.cn (S.C.)

O13-Geopolymer/Zeolite P Composites from Combustion By-products

A. Chuwongwittaya[1], A. Siyasukh[1] and K. Pimraksa[1, 2, ‡]

[1]*Department of Industrial Chemistry, Faculty of Science, Chiang Mai University, 50200, Thailand*

[2]*Center of Excellence in Materials Science and Technology, Faculty of Science, Chiang Mai University, 50200, Thailand*

This research paper investigated the synthesis of geopolymer/zeolite composites from lignite fly ash and biomass ash using combined reactions of geopolymerization and zeolitization under hydrothermal treatment. The initial molar ratios of SiO_2/Al_2O_3 were designed in the range of 3.0-6.0 using different hydrothermal alkalinities, hydrothermal temperature and time, and specimen preparation in hydrothermal system. At low SiO_2/Al_2O_3 molar ratio (3.0-5.0), sodalite zeolite could be obtained incorporating with geopolymeric phase. Tobermorite binder was also formed in this range. Zeolite P was found at higher SiO_2/Al_2O_3 molar ratio (4.0-5.0). The formation of zeolitic materials in geopolymeric matrix affected a mechanical strength of the hardened composite materials. At SiO_2/Al_2O_3 molar ratio of 5.0 before hydrothermal treatment, geopolymeric gel was mainly formed reaching the highest compressive strength and density about 43.5 MPa and 1.91 g/cm^3 respectively. The strength degraded over 50% to be 19.0 MPa after hydrothermal treatment that related to the density of 1.73 g/cm^3 owning to the formation of geopolymeric/zeolite composite.

Keywords: Geopolymer, Zeolite, Hydrothermal method, Waste circulation

Email: ‡kedsarin.p@cmu.ac.th

O14-Orbital two-channel Kondo effect in antiferromagnetic Weyl semimetal Mn_3Ge

X. Y. Yao, G. X. Cao*
Materials Genome Institute, Shanghai University, Shanghai, 200444, China

Topological state becomes an important part of condense matter systems, but previous focus has been on weak electron correlation systems. Weyl semimetals in strong correlation system is a fascinating platform to research interaction between interesting topological state and the complicate Kondo effect. Here we report the orbital two-channel Kondo (2CK) effect in antiferromagnetic Weyl semimetal Mn_3Ge single crystals, where three regimes of temperature dependence with a hallmark $-T^{1/2}$ dependent non-Fermi liquid behavior and H independence in longitudinal resistivity were experimental observed. Weak ferromagnetism (M_S=18 mμ_B/f. u.) does not break the symmetry of channel. Moreover, we discover a crossover between non-Fermi liquid and Landau-Fermi liquid behaviors at low temperature energy scale. This finding manifests the two-level systems driven 2CK physics. Our results prove the presence of orbital two-channel Kondo physics in magnetic Weyl semimetals with certain spin polarization.

Keywords: Weyl semimetals, Orbital two-channel Kondo effect, Strong correlation
Email: guixincao@shu.edu.cn

O15-Effect of Sn on Segregation Behavior of Si during Solidification of Molten Steel

N. Jinno[1], K. Kato[2], and H. Ono[2]‡

[1]*Graduate School of Science and Engineering, University of Toyama, Toyama 930-8555, Japan*

[2]*Academic Assembly, Faculty of Sustainable Design, University of Toyama, Toyama 930-8555, Japan*

Steel scraps recovered from the society contain tramp elements, which are difficult to remove once they dissolve in molten iron. Sn, used as a solder for electronic devices and tin plates, is one of the significant tramp elements. Because Sn is difficult to remove in the refining process, Sn remains to exist in molten steel and affects the behavior of the other elements during the solidification process due to the thermodynamic interaction between Sn and other elements. Consequently, in order to produce high-quality steel, it is necessary to understand and control the effect of Sn on the other elements. On the other hand, the Si content of high tensile strength steels, such as transformation-induced plasticity steel (TRIP steel), is precisely controlled to achieve high strength and high elongation. However, Si and Sn are concentrated in the liquid phase during solidification. Therefore, segregation behavior of Si can be changed due to the thermodynamic interaction between Si and Sn. Therefore, this study aims to understand the effect of Sn on the segregation behavior of Si in the solidification process of Fe-3%Si-0.5%C-0.4%Mn alloy. The unidirectional solidification experiment of the Fe-3%Si-0.5%C-0.4%Mn(-0.5%Sn) alloy was conducted using a horizontal electric resistance furnace with a temperature gradient. The sample was heated to 1873 K and held for 2 h. Subsequently, the sample was cooled at a constant cooling rate under the temperature gradient. The sample was cut in a parallel direction to the solidification direction. The sample cross-section was polished and etched in nitric acid or nital. The macro- and micro-structures of the cross-section were observed by optical microscopy and scanning electron microscopy (SEM). Si and Sn content distribution was analyzed by an energy dispersive X-ray spectroscopy (EDS). The results showed that Si and Sn are concentrated together at the end of the solidification.

Keywords: Solidification, Steel, Tramp elements

Email: ‡ono@sus.u-toyama.ac.jp

O16- The spin-switching and magnetocaloric research in Tb doped $YbFeO_3$ single crystal

W. T. Yang[1], S. Zhu[1], X. X. Ma[1], B. J. Kang[1], J. K. Bao[1], S. X. Cao[1,3*‡]

[1] *Department of Physics, Materials Genome Institute and International Center for Quantum and Molecular Structures, Shanghai University, Shanghai, 200444, China*

[3] *Shanghai Key Laboratory of High Temperature Superconductors, Shanghai University, Shanghai, 200444, China*

Rare earth orthoferrites $RFeO_3$ (where R = rare earth element) often have excellent magnetic, magnetocaloric, and magneto-optical properties. The properties of distinct rare earth elements are frequently varied. $YbFeO_3$ single crystal exhibits spin-switching (SSW) effect and spin reorientation transition (SRT) at low temperatures, but its mediocre magnetocaloric properties limits further applications. Therefore, we doped $YbFeO_3$ with a high concentration of Tb ions at the R site (Yb:Tb = 1:3). The $TbFeO_3$ single crystal shows a giant magnetocaloric effect, but the SSW effect has yet to be reported. By measuring the M-T, M-H curves of $Yb_{0.25}Tb_{0.75}FeO_3$ single crystal, it is found that the SSW effect is regulated in the FCC mode, and the temperature where the SSW occurs is increased by more than 100 K compared with the $YbFeO_3$. A multi-SSW effect appears in the FCW mode due to the complex competing effect of Yb, Tb and Fe sublattices. The fitting yields a strong linear relationship between the critical magnetization, temperature, and magnetic field for steady and metastable states. Arrott Plots are calculated from the isothermal magnetization curve. SRT is a second-order phase transition and the magnetic order of Tb ions is turned into a first-order phase transition. The $-\Delta S_m$-T and RC-T diagram are also calculated, indicating the $-\Delta S_m$ is effectively increased by doping of Tb ions. So that it has great magnetic refrigeration performance. As a result, it can be employed in both magnetic sensing devices and magnetic refrigeration devices.

Keywords: Rare earth orthoferrites, Spin-switching, Magnetocaloric effect

Email: ‡sxcao@shu.edu.cn

O17-Spin and charge density waves in the quasi-one-dimensional KMn_6Bi_5

J. K. Bao[1,2,3], H. B. Cao[4], M. J. Krogstad[1,5], K. M. Taddei[4], C.F. Shi[2], S. X. Cao[2,3], S. H. Lapidus[5], S. V. Smaalen[6], D. Y. Chung[1], M. G. Kanatzidis[1,7], S. Rosenkranz[1], O. Chmaissem[1,8]

[1]*Materials Science Division, Argonne National Laboratory, Lemont, Illinois 60439, USA*

[2]*Department of Physics, Materials Genome Institute and International Center for Quantum and Molecular Structures, Shanghai University, Shanghai 200444, China*

[3]*Shanghai Key Laboratory of High Temperature Superconductors, Shanghai University, Shanghai 200444, China*

[4]*Neutron Scattering Division, Oak Ridge National Laboratory, Oak Ridge, Tennessee 37831, USA*

[5]*Advanced Photon Source, Argonne National Laboratory, Lemont, Illinois 60439, USA*

[6]*Laboratory of Crystallography, University of Bayreuth, Bayreuth 95447, Germany*

[7]*Department of Chemistry, Northwestern University, Evanston, Illinois 60208, USA*

[8]*Department of Physics, Northern Illinois University, DeKalb, Illinois 60115, USA*

Using neutron diffraction, we elucidate the exact nature of the previously unknown AFM ground state of KMn_6Bi_5 and report finding transverse incommensurate spin density waves (SDWs) for the Mn atoms with a propagating direction along the chains. The SDWs have distinct refined amplitudes of ~2.46 m_B for the Mn atoms in the pentagons and ~0.29 m_B with a large standard deviation for Mn atoms at the center between the pentagons. The SDWs exhibit both local and itinerant characteristics potentially due to cooperative interactions between local magnetic exchange and conduction electrons. Single crystal x-ray diffraction below the AFM transition revealed satellite peaks originating from charge density waves (CDW) along the chain direction with a **q**-vector twice as large as that of the SDW, pointing to a strong real space coupling between them. Our work not only reveals a fascinating intertwined spin, charge, and lattice, orders in one-dimensional KMn_6Bi_5, but also provides an essential piece of information on its magnetic structure to understand the mechanism of superconductivity in this new Mn-based family.

Keywords: Spin/Charge density wave, Quasi-one-dimensional, Mn-based superconductor

Email: chmaissem@anl.gov

O18-Effect of Nb content on the microstructure and corrosion resistance of $FeCoCrNiNb_x$ high entropy alloy in chloride ion environment

C. Liu[1], Y. Gao[1], K. Chong[1], F.Q. Guo[1], D. T. Wu[2], Y. Zou[3]

[1]*School of Materials Science and Engineering, Shandong University, Jinan 250061, China*

[2]*Key Laboratory of Liquid-Solid Structural Evolution and Processing of Materials, Ministry of Education, Shandong University, Jinan, 250061, China*

[3]*Shandong Engineering & Technology Research Center for Modern Welding, Shandong University, Jinan, 250061, China*

In this paper, $FeCoCrNiNb_x$ high entropy alloy was prepared by vacuum arc melting, and the effect of Nb content on its microstructure and corrosion resistance in a chloride ion environment was investigated. Based on the calculated pseudo-binary phase diagram analysis and experimental results show that the microstructure of the FeCoCrNi alloy is a single FCC solid solution and that the Laves phase in the FeCoCrNiNb x alloy increases with the addition of Nb elements, the microstructure of the $FeCoCrNiNb_{0.15}$ alloy is dissociated eutectic, the microstructure of the $FeCoCrNiNb_{0.33}$ alloy is typically sub-eutectic and the microstructure of the $FeCoCrNiNb_{0.5}$ alloy is typically eutectic. The $FeCoCrNiNb_x$ (x=0,0.15,0.33,0.5) alloy has a higher corrosion resistance than the conventional corrosion-resistant 316L stainless steel and the $FeCoCrNiNb_{0.15}$ alloy shows the best excellent corrosion resistance. The FeCoCrNiNb x (x=0.33,0.5) alloy suffers from more severe galvanic corrosion due to the formation of more Laves phases, while the FeCoCrNi alloy and the $FeCoCrNiNb_{0.15}$ alloy benefit from the protection of a dense and stable passivation film with only minor pitting corrosion. The XPS analysis and Mott-Schottky test of the passivation films showed that the solid solution of a small amount of Nb promoted the more formation of dense Cr_2O_3 in the passivation film of $FeCoCrNiNb_{0.15}$ alloy, and the formed passivation film had the characteristics of P-N junction, and compared with the passivation film of FeCoCrNi alloy with mainly n-type semiconductor characteristics, the corrosion resistance of the $FeCoCrNiNb_{0.15}$ is superior.

Keywords: $FeCoCrNiNb_x$ high-entropy alloy, Microstructure, Passivation film, Mott-Schottky curve, Corrosion resistance

E-mail: yzou@sdu.edu.cn

O19-Thermal stability and corrosion behavior of a novel $Zr_{22.5}Ti_{22.5}Hf_{22.5}Ni_{22.5}Ta_{10}$ high-entropy amorphous alloy

K. Chong[1], Y. Gao[1], Z. B. Zhang[1,2], Y. Zou[1‡], X. B. Liang[1,2‡]

[1]*Key Laboratory for Liquid-Solid Structural Evolution and Processing of Materials, Ministry of Education, School of Materials and Engineering, Shandong University, Jinan 250061*

[2]*Defense Innovation Institute, Academy of Military Sciences, Beijing, 100071*

High-entropy amorphous alloys have aroused the interest of researchers due to their unique and excellent properties caused by composition and structure. The present study reasonably designed and prepared a novel $Zr_{22.5}Ti_{22.5}Hf_{22.5}Ni_{22.5}Ta_{10}$ high-entropy amorphous alloy with excellent thermal stability and corrosion resistance. The microstructure of as-spun ribbon was disorder amorphous structure confirmed by XRD and TEM. The DSC test measured that the glass transition temperature (T_g) and crystallization onset temperature (T_x) were 745 K and 812 K, respectively. This high-entropy amorphous alloy showed a wider crystallization range than conventional amorphous, benefiting from the high mixing entropy effect. In addition, the corrosion resistance and passivation behavior of $Zr_{22.5}Ti_{22.5}Hf_{22.5}Ni_{22.5}Ta_{10}$ high-entropy amorphous alloy were carefully investigated. The electrochemical tests confirm better corrosion resistance of $Zr_{22.5}Ti_{22.5}Hf_{22.5}Ni_{22.5}Ta_{10}$ high-entropy amorphous alloy than 316L stainless steel. The excellent corrosion resistance of high-entropy amorphous alloy is attributed to the complex composition and dense structure of the passivation film. The ribbon presents the best corrosion resistance after potentiostatic polarization with the potential of 0 V_{SCE}, and XPS results show the passivation film is mainly composed of the oxides of Zr, Ti, Hf, Ta. Kinetic factors may have contributed to the fact that the measured content of these oxides differed from the thermodynamic tendency to generate them. The semiconducting bipolarity of passivation film is also beneficial to improving corrosion resistance.

Keywords: high-entropy metallic glass, Thermal stability, Corrosion resistance, Passivation film

Email: ‡yzou@sdu.edu.cn

ICPMAT 2022 Shanghai 中国
16th International Conference on the Physical Properties and Application of Advanced Materials
21st-23rd November, 2022

O20-The microstructure and magnetic properties of Fe ion doped $GdCrO_3$

C. F. Shi[1,2], Y. L. Su[2,3], G. S. Gong[2,3], J. K. Bao[1,4*], S. X. Cao[1,4†]

[1]*Department of Physics, Materials Genome Institute and International Center for Quantum and Molecular Structures, Shanghai University, Shanghai 200444, People's Republic of China*

[2]*School of Physics and Electronic Engineering, Zhengzhou University of Light Industry, Zhengzhou 450002, People's Republic of China*

[3]*Henan Key Laboratory of Magnetoelectronic Information Functional Materials, Zhengzhou University of Light Industry, Zhengzhou 450002, People's Republic of China*

[4]*Shanghai Key Laboratory of High Temperature Superconductors, Shanghai University, Shanghai 200444, People's Republic of China*

The evolution of microstructure and magnetic properties of $GdCrO_3$ systems were investigated with the substitution of Fe in Cr site via solid state reaction method. X-ray diffraction and Fourier transform infrared spectra characterization analyses show that the $GdCr_{1-x}Fe_xO_3$ ($0 \leq x \leq 0.5$) polycrystalline samples were successfully prepared, the lattice constants and CrO_6 octahedral deformation increase with the Fe doped concentration. Positron annihilation spectra indicate a decrease in defect volume and an enhancement of defect concentration with the introduction of Fe. Simultaneously, the field-cooled (FCC) and zero-field cooled (ZFC) curves of $GdCr_{1-x}Fe_xO_3$ ($0 \leq x \leq 0.5$) samples exhibit that the magnetization reversal of $GdCrO_3$ can be inhibited after the Fe introduced into the lattice, and FCC curves show spin flip characteristics due to the anomalous lattice distortion at $x = 0.3$ and $x = 0.4$ sample. Additionally, the antiferromagnetic temperature (T_N) varies with strength of symmetric (J_e).

Keywords: Microstructure, Spin flip, Vacancy defect

Email: *jinke_bao@shu.edu.cn, †sxcao@shu.edu.cn

O21-Surface modification of aluminum alloy by local laser irradiation

A. Saiki[1]*, M. Yamamoto[1], T. Hashizume[1]

[1]*Department of Materials Design and Engineering, School of Sustainable Design, University of Toyama, Toyama, Japan*

Aluminum is lightweight, has high specific strength, and is highly decorative, so demand for aluminum will continue to increase in the transportation, construction, and home appliance industries. While smelting from ore requires a large amount of energy, recycling requires a smaller amount of energy, and the percentage of recycled materials will increase in the future from the viewpoint of energy consumption, including CO2 emission limits. In recycled aluminum alloy materials with a relatively high proportion of unintended constituents, surface properties and their modification as well as strength will become important in the future.

In this study, we attempted to modify the strength and surface properties of the material by utilizing the ability of laser irradiation to selectively heat only a few microns in size to modify the local area near the surface. By applying the laser heat treatment to the material surface in an arbitrary irradiation pattern, it was possible to create a microstructure with different thermal histories at different locations. As a result, the laser-patterned aluminum alloy materials showed anisotropic mechanical properties, and at the same time, the surface condition of the material was affected.

Keywords: Laser irradiation, Aluminum alloy, Anisotropy, Hardness

Email: saiki@sus.u-toyama.ac.jp

O22-Flux pinning behavior and related physical mechanism of $CaKFe_4As_4$ superconductor

T. He[1,2], C. L. Wang[2], J. Y. Ge[1]

[1]*Materials Genome Institute, Shanghai University, Shanghai 200444, People's Republic of China*

[2]*Key Laboratory of Microelectronics and Energy of Henan Province, Henan Joint international Research Laboratory of New Energy Storage Technology, School of Physics and Electronic Engineering, Xinyang Normal University, Xinyang 464000, People's Republic of China*

We have synthesized iron-based superconductor $CaKFe_4As_4$ single crystals by a simple one-step method, the onset transition temperature is about 35 K with the ΔT_c ~1 K. By measuring the magnetoresistance and dynamical magnetization relaxation, the vortex transitions of the $CaKFe_4As_4$ single crystals have been investigated, a small region of vortex liquid region is observed indicating strong flux pinning ability. The J_c can be respectively enlarged more than 3 and 50 times in H parallel to c-axis and ab-plane at temperature of 5 K and high magnetic fields of 8 T when the d is reduced from 88 to 2.0 μm. Accompanied by the enhanced J_c, the fishtail effect fades away with the decreasing d, both the origins of enhanced J_c and the fishtail effect in $CaKFe_4As_4$ may have close relationship with the interlayer coupling between $CaKFe_4As_4$ and the intercalations of KFe_2As_2. Based on the dynamic relaxation rate Q and transient current J_s by means of generalized inversion scheme, the pinning mechanisms of $CaKFe_4As_4$ with different defect types have been studied, it seems that non-superconducting second phase with the size close to ξ are necessary to obtain strong δT_c-pinning in $CaKFe_4As_4$. The present work illustrates how the defect structure affects the flux pinning behaviors and can provide a new clue to design high-performance superconducting wire/tapes and films for strong magnetic field applications.

Keywords: Iron-based superconductor, Flux pinning, Defect structure

Email: hetian0928@shu.edu.cn

ICPMAT 2022 Shanghai 中国
16th International Conference on the Physical Properties and Application of Advanced Materials
21st-23rd November, 2022

O23-Effect of thermal aging on the properties and microstructure of Al-Cu-Mg-Si alloy

V. N. Hai, H. Saito[1], T. Tsuchiya[2], S. Lee[2], S. Ikeno[3], T. Katsumi[4], K. Kita[4], K. Matsuda[2, †]

[1]*Graduate School of Science and Engineering, University of Toyama, Toyama, Toyama, 930-8555, Japan*

[2] *Faculty of Sustainable Design, Department of Materials Design and Engineering, University of Toyama , Toyama, Toyama, 930-8555, Japan*

[3]*Professor emeritus, University of Toyama, Toyama, Japan*

[4]*YKK CORPORATION, Kurobe, Toyama 938-8601, Japan*

The 2XXX series alloys are heat treatable aluminum alloys based on the Al-Cu-Mg-(Si) system. They are used in high-performance structural aerospace and transportation application. In this study, the effects of solution and aging treatments on the microstructure and mechanical properties of Al-1.0Cu-0.96Mg-0.36Si alloy were investigated. The sample was then cut into smaller pieces, heat treated, grinded and polished before performing hardness test and observing the precipitation distribution in microstructure. The objective of present work is to establish the hardness and ageing time curve, microstructure examination for different heat treatment conditions was observed and optimization of the heat treatment was done with a more detailed understanding of the precipitation process .The results show that it is possible to reach a high level of hardness within a short period of time as compared to diverse conditions. The 2-step aging process is also analyzed to compare peak age period and hardness level of the material, 2-step aging are then compared with the three different cold-rolling in reduction to conclude which has the most suitable peak hardness for commercial use. The enhancement of properties after aging is attributed to the precipitation of β'', $S''$and θ'' phase from the α-Al matrix. When an aluminum alloy is used, forming is one of the indispensables processes, and dislocation and grain refinement occurring during processing have a great influence on the formation of precipitation. In this study, the effect of pre-aging temperature and cold colling processing on the 2-step aging of the Al-1.0Cu-0.96Mg-0.36Si alloy will be investigated using transmission electron microscopy(TEM) to investigate the effect of precipitation process and precipitation on strength improvement.

Keywords: 2-step aging process, Precipitation, TEM

Email: †ikenolab@sus.u-toyama.ac.jp

O24-Electric transport properties of ZrB_{12} micro-bridge

A. L. Zhang[1], L. X. Gao[1], J. Y. He[1], V. B. Filipov[2], Q. L. Xiao[1], J. Y. Ge[1, 3, 4, ‡]

[1]*Materials Genome Institute, Shanghai University, 200444 Shanghai, China*

[2]*Frantsevich Institute for Problems of Materials Science, NASU, 03680 Kiev, Ukraine*

[3]*Department of Physics, Shanghai Key Laboratory for High Temperature Superconductors, Shanghai University, 200444 Shanghai, China*

[4]*Zhejiang Laboratory, Hangzhou, 311100, China*

ZrB_{12} single crystal has controversies in its band and superconductor type [1-3]. New experiments have already show evidence of type 1.5 and two-band superconductor [4-5]. Theoretical analysis suggests that decreasing thickness could cause a transition of superconductor type to a type II superconductor from a type 1.5 or type I superconductor, which may mean that the weak influence of two band structure. In our experiments, the ZrB_{12} micro-bridge with 1μm thickness was prepared by focused ion beam. Then the resistivity and *I-V* measurements were carried out using the standard four-dc-probe technique. *R-T* curves of higher magnetic fields show "knees" at lower temperatures, which is the classical character of 2 dimension (2D) superconducting phase and also show a quantum phase transition to an intermediate 2D metallic state, Bose metal, with a resistance much lower than R_N. The activated energy deduced from *R-T* curves presents two separated stages. The *I-V* measurement shows the existence of the Berezinskii-Kosterlitz-Thouless (BKT) transition, which represents the motion of the free vortices. However it does not show hysteresis in the *I-V* curves, which is also the critical symbol of 2D superconducting phase. Instead it shows a slight step in the *I-V* curves especially at low temperature and low magnetic field. So the ZrB_{12} micro-bridge may have a quasi-2D superconducting state and is possibly influenced by the two band structure with two different coherence length (ξ). From the *I-V* curves, critical current (J_c) of ZrB_{12} micro-bridge was extracted. The penetration depth (λ) deduced from J_c cannot be fitted by a single band. Although type 1.5 superconductor ZrB_{12} presents a single λ, it can be influenced by its two band structure. The fitting of extracted λ with two-band model suggests that below 4.9 K, both the lower band and higher band play the role at the same time and above 4.9 K the higher band play the vital role. The results of our experiments suggest that the two-band structure still has a vital role on the superconductivity of ZrB_{12} micro-bridge with a possible state of quasi-2D superconducting.

Keywords: Type 1.5 superconductor, Quasi-2D superconducting, Electric transport

Email: ‡ junyi_ge@t.shu.edu.cn

O25-Data-driven techniques for high-hardness Al-Mg-Si series alloy to obtain optimal chemical composition

Y. Koishikawa[1], N. Nunomura[2], T. Nakamura[1]

1*Graduate School of Science and Engineering for Education, University of Toyama, Toyama, Japan*

2*Graduate School of Science and Engineering for Research, University of Toyama, Toyama, Japan*

In conventional alloy development, many scientists have successfully made major discoveries by conducting experiments based on their own experience and intuition. However, these approaches require enormous amounts of time and money, and depend on researcher's experiences. At the same time as this study, various researchers have proposed by machine learning to develop aluminum alloys, but no one have been reported utilizing mathematical optimization. Therefore, we proposed the new method about alloy development with machine learning and mathematical optimization. To create an experimental dataset, we collected data on alloy compositions and their hardness from papers. Multiple regression analysis was performed to predict hardness form chemical composition, using Wrapper Method for variable selection and Leave-One-Out cross validation for data division. To examine the prediction accuracy of our model, we applied the coefficient of determination (R^2) and root mean square error (RMSE), and then the values were 0.770 and 12.51 [HV], respectively. Furthermore, by combining machine learning results with mathematical optimization, the optimal alloy composition can be obtained. Result of mathematical optimization will be reported in detail on the day.

Keywords: Data-driven, mathematical optimization, Al-Mg-Si series alloy

Email: ‡m2171513@ems.u-toyama.ac.jp

O26-Phase diagram for $Fe_ySe_xTe_{1-x}$ superconductors

J. Y. Zhang, J. Y. Ge‡

Materials Genome Institute, Shanghai University, Shanghai 200444, People's Republic of China

Because of its simple crystal structure and abundant phase diagrams, Fe(Se, Te) is considered as an ideal candidate to study the superconducting mechanism of iron-based superconductors, and even high-temperature superconductors. The superconductivity of Fe(Se, Te) is sensitive to its compositional variation, not just the Se content, but also the Fe content. Several Se content-dependent electronic and magnetic phase diagrams for Fe(Se, Te) superconductors have been established, but the Fe content-dependent phase diagram is still absent. Here, a series of $Fe_ySe_{0.4}Te_{0.6}$ bulks has been fabricated by the solid state reaction method and corresponding thin films have also been prepared by the pulsed laser deposition method. The effect of Fe content, in the range of 0.6 to 2.0, on the structure and superconductivity of $Fe_ySe_{0.4}Te_{0.6}$ superconductors has been systematically investigated, and a more complete phase diagram for $Fe_ySe_xTe_{1-x}$ superconductors with wider range of Fe content was developed. When Fe content is taken into account, the Se content x corresponding to $Fe_ySe_xTe_{1-x}$ film with the highest superconducting transition temperature (T_c) shifts to a lower value, instead of 0.8. Our results provide a more accurate phase diagram for the Fe(Se, Te) superconductors, which facilitates the rational regulation of the superconducting properties, as well as the study of the underlying superconducting mechanism.

Keywords: $Fe_ySe_xTe_{1-x}$ superconductors, Fe content, Phase diagram

Email: ‡junyi_ge@t.shu.edu.cn

O27-Thermophysical and mechanical properties of Al2O3-doped YTaO4 ceramic as potential thermal barrier coating

T. Xue[1], Y. Zou[2]

[1]*School of Materials Science and Engineering, Shandong University, Jinan, Shandong, 250061, China*

[2]*Shandong Engineering & Technology Research Center for Modern Welding, Shandong University，Jinan, Shandong, 250061, China*

In this paper, a series of solid solutions ceramics of (AlxY1-x)TaO_4 (x = 0, 0.02, 0.04, 0.06, 0.08, 0.1) were synthesized via hot pressing solid-state reaction, after which an analysis of the phase composition and microstructures of the samples is conducted using X-ray diffraction (XRD), Raman spectroscopy and scanning electron microscopy (SEM). X-ray photoelectron spectroscopy (XPS) employed to characterize the variation of bond energy with composition reveals that Al3+ ions substitute Y3+ ions in the structure of YTaO4 ceramics. The thermal expansion coefficients (TECs) of (AlxY1-x)TaO_4 ceramics vary in some ranges (10–11.5 × 10−6 K−1, at 1200 °C), but are comparable to that of YSZ. In addition, this research systematically investigates the discipline of hardness and modulus changing with the composition. Given the excellent thermophysical properties it exhibits, (AlxY1-x)TaO_4 ceramic material is believed to be a prospective TBCs material.

Keywords: Ceramics, TBCs, Rare earth tantalates, Thermal properties, Mechanical property

Email: yzou@sdu.edu.cn

O28-Interfacial and opto-electronic properties of halide perovskites: from toxic to eco-friendly

S. H. Wang

Materials Genome Institute, Shanghai University, Shanghai 200444, China

Recent years, the organic-inorganic hybrid perovskite solar cells (PSCs) have attracted extensive attention due to their intriguing optoelectronic properties. The power conversion efficiency (PCE) has increased from 3.8% to 25.7%, which reveals very promising potential for commercial applications. In this presentation, I will present the interfacial and opto-electronic properties of all-inorganic cesium lead halide perovskite (CsPbI3), as well as the method for preparing high-performance device. The growth dynamics of CsPbI3 perovskite and a detailed study on hole transport material for CsPbI3 to enhance the stability and the opto-electric conversion efficiency will also be discussed. Lead-based perovskites deliver excellent device performances, but Pb is a toxic element. To avoid the health crisis to human beings and the pollution to our environment, it is essential to develop non-toxic perovskites. Alternatively, Sn-based perovskites show the merit of eco-friendliness. The growth of CsSnI3 and the challenges will be discussed.

Email: shenghaowang@shu.edu.cn

O29-Field-driven surface state and topological nodal lines in layered semimetals

G. X. Cao *

Materials Genome Institute, Shanghai University, Shanghai, 200444, China

The metallic surface state of topological insulators (TI) are protected by the time reversal symmetry (TRS). The Hallmark of the universal metallic surface state in the transport is a clear resistivity plateau at low temperatures in ideal TI or in several three-dimensional (3D) and two dimensional (2D) topological semimetals when breaking TRS. However, the observation of topological surface in the low-dimensional are scare. We report experimental evidence of topological surface state in the quai-one-dimensional (Q1D) and 2D van der Waals semimetals. Magnetotransport measurements display the emergency of a field induced low-temperature (low-T) topological insulator (TL) with a plateau. Combined angle-resolved photoemission spectroscopy (ARPES) and density functional theory (DFT) calculations reveals multiple Dirac nodal lines, with a small gap opening in the spin-orbit coupling.

Keywords: Topological semimetals, Nodal lines, Van der Waals.

Email: guixincao@shu.edu.cn

O30-Improvement on electrochemical activity of anode materials for magnesium rechargeable batteries by laser processing

T. Tsukeda[1], K. Kikura[2], T. Aida[1], H. Tabat[3], H. Kurihara[4], and M. Suzuki[5]

[1]*University of Toyama, Faculty of Sustainable Design, Toyama, 930-8555, Japan*

[2]*University of Toyama, Graduate School of Science and Engineering, Toyama, 930-8555, Japan*

[3]*Chuetsu Metal Works Co., Ltd., Advanced Technology Laboratory, Toyama, 930-0298, Japan*

[4]*Saitama Industrial Technology Center (SAITEC), Saitama, 333-0844, Japan*

[5]*Toyama Prefectural University, Faculty of Engineering, Toyama, 939-0398, Japan*

The social implementation of innovative rechargeable batteries is urgently needed in various fields. In particular, magnesium is attracting attention from the viewpoint of cost, safety, and electric capacity, which are the issues of conventional lithium-ion batteries. The authors have focused on the single roll rapid solidification method to reduce production costs, and have found that the electrochemical activity of Mg-3mass%Al-1mass%Zn (AZ31) alloy and Mg-5.3mass%Al-3mass%Ca (AX53) alloy in ribbons on the order of 0.1mm in thickness surpassed that of conventional AZ31 rolled materials used for Mg rechargeable batteries. To further improve the properties, the electrochemical activity of Mg-Al-Ca alloy ribbons and AZ31 rolled material was investigated by drilling with an ultrashort laser pulse to enhance the charge-discharge reaction by increasing the surface area.

For the Mg-Al-Ca alloys used as specimens, Ca was kept constant at 3% and Al was varied from 0 to 14%. The melting points of the alloys were calculated using Thermo-Calc. The single roll type liquid quenching and solidification apparatus uses oxygen-free copper cooling rolls, and the material in a crucible with a nozzle made of SUS430 is heated and melted by a high-frequency coil and injected with Ar gas onto a high-speed rotating roll to produce a ribbon. The redox behavior of magnesium alloys as electrochemical activity was evaluated by constant-current charge-discharge tests using a three-pole Beaker cell. The working electrode was a ribbon sample, the counter electrode was an activated carbon electrode, the reference electrode was a high-purity magnesium foil, and the electrolyte was a cyclic acid anhydride, succinic anhydride: SA and MgTFSA2 dissolved in DMA. A high-power femtosecond oscillation laser was used to process the free-solidification surface of the composition thin zone, which had the best electrochemical activity. The processing conditions for the holes were the most filled array, a hole diameter of 0.06 mm, and a hole center-to-center distance of 0.08 mm. Addition of 3%Ca alone to pure Mg caused a rapid increase in polarization resistance, but combined addition with Al reduced the overvoltage, and combined addition of 9%Al (AX93) showed excellent electrochemical activity. However, a higher excess of Al had the opposite effect. Therefore, laser processing was performed on an AX93 ribbon and an AZ31 rolled plate as a comparison material.

First, the patterns were found to have a larger surface area in the tightly packed configuration than in the simple cubic configuration. Furthermore, the combination of hole diameter and center-to-center distance

can be expected to increase the surface area by a factor of up to 4, but this time a prototype was made with a diameter of 60 μm and center-to-center distance of 80 μm (aiming for a 2.6-fold increase in surface area). Both the AX93rribbon and AZ31 rolled material samples showed an increase in activity of about 200 mV.

Keywords: magnesium rechargeable batteries, Single roll rapid solidification method, Laser processing, Mg-Al-Ca alloy ribbons

Email: tsukeda@sus.u-toyama.ac.jp

O31-Electronic structure of FeS superconductor

J. Miao[1], X. H. Niu[1], D. F. Xu[1], Q. Yao[1], Q. Y. Chen[1], T. P. Ying, [1] S. Y. Li[1,2], Y. F. Fang[3], J. C. Zhang[3], S. Ideta[4], K. Tanaka[5], B. P. Xie[1,2], D. L. Feng[1,2,†], and F. Chen[3,‡]

1*State Key Laboratory of Surface Physics, Department of Physics, and Laboratory of Advanced Materials, Fudan University, Shanghai 200433, People's Republic of China*

2*Collaborative Innovation Center of Advanced Microstructures, Nanjing, 210093, China*

3*Materials Genome Institute, Shanghai University, Shanghai 200444, People's Republic of China*

4*UVSOR Synchrotron Facility, Institute for Molecular Science, National Institutes of Natural Science, Myodaiji, Okazaki 444-8585, Japan*

5*UVSOR Synchrotron Facility, Institute for Molecular Science, Myodaiji, Okazaki 444-8585, Japan*

Here we report the electronic structure of FeS, a recently identified iron-based superconductor. Our high-resolution angle-resolved photoemission spectroscopy studies show two holelike (α and β) and two electronlike (η and δ) Fermi pockets around the Brillouin zone center and corner, respectively, all of which exhibit moderate dispersion along k_z. However, a third holelike band (γ) is not observed, which is expected around the zone center from band calculations and is common in iron-based superconductors. Since this band has the highest renormalization factor and is known to be the most vulnerable to defects, its absence in our data is likely due to defect scattering—and yet superconductivity can exist without coherent quasiparticles in the γ band. This may help resolve the current controversy on the superconducting gap structure of FeS. Moreover, by comparing the β bandwidths of various iron chalcogenides, including FeS, $FeSe_{1-x}S_x$, FeSe, and $FeSe_{1-x}Te_x$, we find that the β bandwidth of FeS is the broadest. However, the band renormalization factor of FeS is still quite large, when compared with the band calculations, which indicates sizable electron correlations. This explains why the unconventional superconductivity can persist over such a broad range of isovalent substitution in $FeSe_{1-x}Te_x$ and $FeSe_{1-x}S_x$.

Keywords: Electronic structure, Iron-based superconductor, ARPES

Email: ‡chf001@t.shu.edu.cn

ICPMAT 2022 Shanghai 中国
16th International Conference on the Physical Properties and Application of Advanced Materials
21st-23rd November, 2022

O32-Improving CMAS-corrosion resistance of YSZ-based thermal barrier coatings with Al_2O_3 addition

J. S. Han[1], Y. Zou[1], D. T. Wu[1], J. Chen[1], Y. G. Zhang[1,2]

[1]*Key Laboratory for Liquid-Solid Structural Evolution and Processing of Materials, Ministry of Education, Shandong University, Jinan 250061, PR China*

[2]*Shenzhen Research Institute of Shandong University, Shenzhen 518063, PR China*

Thermal barrier coatings (TBCs), exposed to the molten calcium-magnesium-aluminum-silicate (CMAS) deposits, could become degraded more readily during service. In this paper, the composite Al_2O_3/YSZ TBCs with different Al_2O_3 additions were prepared through the atmospheric plasma spraying technique and their resistance to CMAS corrosion at 1250 ℃ was carefully compared to the 7YSZ (7 wt.% Y_2O_3 stabilized ZrO_2) TBCs. It was found that two distinct microstructural characteristics, i.e. thermo-chemical reaction zone and CMAS physical-infiltration zone, were identified for both the 7YSZ coating and the 10 wt.% Al_2O_3-7YSZ coating. The thermo-chemical reaction zone was severely corroded by molten CMAS, inducing the dissolution and re-precipitation of YSZ material and generating small globular m-ZrO_2 particles. Furthermore, these two coatings were completely infiltrated (approximately 300 μ m) and developed significant macroscopic bending. With the Al_2O_3 addition increasing above 20 wt.%, the depth of the thermo-chemical reaction zone was restricted to 35 μ m without obvious CMAS physical-infiltration. During CMAS attacking the Al_2O_3/YSZ coating, continuous dissolution of Al_2O_3 into CMAS melt could promote anrthite crystallization along the CMAS-coating interface, which effectively restrained CMAS penetration and improved CMAS corrosion resistance.

Keywords: Thermal barrier coatings, Atmospheric plasma spraying, Al_2O_3/YSZ composite coating, CMAS corrosion

Email: jiasenhan@sina.com

O33-In-situ conversion of amorphous carbon to graphene enhances the oxidation resistance of dendritic copper powder

M. Q. Zhang[1,2], G. X. Cao [1,*], J. C. Zhang[1,*], Q. X. Ye [2,*] , Y. L. Huang[1], X. Y. Yao[1], R. D. Yu[2], J. Wang[2], Z. C. Xiao[2], L. X. Zhou [2,*], J. M. Cai [2,*]

[1]Materials Genome Institute, Shanghai University, Shanghai 200444, People's Republic of China

[2]Faculty of Materials Science and Engineering, Kunming University of Science and Technology, Kunming 650093, People's Republic of China

Copper powder has excellent electrical conductivity, but is easily oxidized by air. This limits its application in printed circuits and related fields. In this paper, graphene was grown in-situ on the surface of dendritic copper powder in order to improve the powders' oxidation resistance and maintain its high electrical conductivity. Firstly, dendritic copper powder with a diameter of about 100-200 nm was prepared by electrochemical deposition. Then, the powder was coated with an amorphous carbon film by Plasma Enhanced Chemical Vapor Deposition (PECVD) using C_2H_2 at 350℃. Finally, the amorphous carbon film was transformed into graphene at 850℃, and dendritic copper powder coated with graphene was obtained. TG-DTA and electrical resistivity measurements showed that the oxidation resistance temperature of dendritic copper powder can be increased from 213.7 ℃ to 283.4 ℃ and the resistivity can be reduced from 0.00544 Ω·cm to 0.00308 Ω·cm by in-situ growth of graphene on the surface of copper powder. The in-situ synthesis of graphene is expected to promote the wide application of copper powder in areas requiring high electrical conductivity and oxidation resistance.

Keywords: Dendritic copper powder, Amorphous carbon, Graphene, Anti-oxidaion

Email: j.cai@kmust.edu.cn.

ICPMAT 2022 Shanghai 中国
16th International Conference on the Physical Properties and Application of Advanced Materials
21st-23rd November, 2022

P1-Effect of Injection Molding Conditions on Dimensional Accuracy and Mechanical Properties of Carbon Fiber Reinforced PEEK

K. Maida[1], T. Nakagawa[2], T. Tsukeda[2], T. Aida[2], Y. Funato[3], and S. Kajikawa[4]

[1]*University of Toyama, Graduate School of Science and Engineering, Toyama, 930-8555, Japan*

[2]*University of Toyama, Faculty of Sustainable Design, Toyama, 930-8555, Japan*

[3]*TC Toyama Co., Ltd., Toyama, 930-0274, Japan*

[4]*Makino Milling Machine Co., Ltd., Kanagawa, 243-0303, Japan*

In recent years, machine tools have been required to achieve higher machining accuracy and productivity. In order to satisfy those requirements, spindle speed and accuracy must be increased. As the spindle speed increases, the rotational speed of the bearings supporting the spindle also increases. When the rotational speed of the bearing increases, the friction between the balls and cage increases in steel cages, causing seizure and cage damage. Therefore, attention has focused on resin cages, which are superior to steel in terms of self-lubrication, low friction, and light weight. Furthermore, super engineering plastics with a heat resistance temperature of 150℃ or higher are increasingly demand as a metal substitute material. The polyether ether ketone (PEEK) used in this study has a high heat resistance of 240°C, and has superior mechanical properties compared to polyamide, which the resin materials that traditionally has been used as a cage material. To improve mechanical properties, 30 wt.% carbon fiber was added to the molding process.

Injection molding is the main molding methods for resin materials. In this study, an in-line screw type injection molding machine was used. This system has a simpler structure than the pre-plunger system, making it easier to maintain, and injection are performed with a single cylinder, resin retention is less likely to occur. Injection molding has the advantages of high productivity, no post-molding processing, and the ability to accommodate complex shapes. However, there are disadvantages such as dimensional defects due to molding shrinkage and reduced strength due to differences in resin flow. Therefore, we investigated the effects of injection molding conditions on the dimensional accuracy and tensile strength of carbon fiber reinforced PEEK in order to improve the properties of resin retainers.

The specimen is a resin material made of PEEK with 30% carbon fiber added. For molding, samples were made using an inline injection molding machine with a mold clamping force of 200 t, a plunger diameter of 28 mm, and a maximum injection pressure of 287 MPa. The molding conditions were set at holding pressures between 0 and 270 MPa. The molded products were evaluated for dimensional accuracy and mechanical properties by measuring roundness using a CNC image measuring instrument and tensile testing at room temperature. In addition, SEM observation of the fracture surface was performed to examine the orientation of the carbon fibers on the fracture surface, the tensile strength also increased.

Keywords: PEEK, Carbon fiber, Injection molding, Roundness, Tensile strength

Email: m10821kei@gmail.com

ICPMAT 2022 Shanghai 中国
16th International Conference on the Physical Properties and Application of Advanced Materials
21st-23rd November, 2022

P2-Organic Lead-based Halide Perovskite Single Crystal for High-performance Photodetector

Y. H. Chen[1,2,3], Z. J. Feng[1,2,3,4*], and J. C. Zhang[1,2*]

[1]*Materials Genome Institute, Shanghai University, Shanghai, 200444, China*
[2]*Zhejiang Laboratory, Hangzhou 311100, China*
[3]*Shanghai Laue Sci. & Tech. Institute, Shanghai, 200444, China*
[4]*Shanghai Key Laboratory of High Temperature Superconductors, Department of Physics, Shanghai University, Shanghai, 200444, China*

There has been growing interest in organic Lead-based halide perovskites as a promising candidate for optoelectronic applications due to their excellent optical and electrical characteristics, such as high and balanced carrier mobility, long carrier diffusion length, and adjustable band gap. Despite this, most of the reported perovskite photodetectors based on polycrystalline thin films suffer immensely from high trap density and poor stability owing to grain boundaries, limiting their photoelectric performance. Perovskite single crystal have the ability to reduce the trap density and construct high performance photodetectors compared to their thin-film counterparts. Herein, we present a new method of using hydrobromic acid as solvent to grow $CH_3NH_3PbBr_3$ single crystal via inverse temperature crystallization. The Au/ $CH_3NH_3PbBr_3$ single crystal/Au photodetector was fabricated, which exhibits a fast rise and decay time of 180 ms and 310 ms under the 450 nm light illumination at 3 V, respectively. We provide an alternative approach for fabricating perovskite single crystal, which could apply to high performance photodetector.

Keywords: $CH_3NH_3PbBr_3$ single crystal, hydrobromic acid, high performance photodetector
Email: fengzhenjie@shu.edu.cn; jczhang@shu.edu.cn

ICPMAT 2022 Shanghai 中国
16th International Conference on the Physical Properties and Application of Advanced Materials
21st-23rd November, 2022

P3-Microstructure evolution of Al-1.0Mg-0.6Si(mass%) alloys with homogenization treatment

S. Kawamata[1], T. Tsuchiya[2], S.Lee[2], S. Ikeno[3], and K. Matsuda[2, †]

[1]Graduate School of Science and Engineering, University of Toyama, Toyama, Toyama, 930-8555, Japan

[2] Faculty of Sustainable Design, Department of Materials Design and Engineering, University of Toyama , Toyama, Toyama, 930-8555, Japan

[3]Professor emeritus, University of Toyama, Toyama, Japan

Al-Mg-Si alloys can be increased strength remarkably with aging treatment. They are widely used as an extrusion material for construction materials and automotive parts. Because they have good specific strength, formability, and corrosion resistance by anodizing. In extrusion process, Al alloys are subjected to homogenization prior to hot extrusion. The homogenization process eliminates and homogenizes micro-segregation formed during casting. Homogenization treatment improves extrusion speed by reducing β-AlFeSi phase and decreases surface defects like “pickups” during extrusion. The mechanism of pickups has been proposed to be influenced by the dissolution of β-AlFeSi and Mg2Si compounds. In the microstructure after casting and homogenization, plate and rod precipitates existed in addition to the intermetallic compounds. These precipitates may be thermodynamically equivalent to the intermetallic compounds or may dissolve at lower temperatures. Even after homogenization treatment, the coarse precipitates were not fully solidified and remained after extrusion. The purpose of this study is to investigate the effect of homogenization on the microstructure after extrusion.Two kinds of alloys were prepared; (1) non-homogenization and (2) with-homogenization treatment at 848K for 7.2ks. Microstructure evolution was investigated each alloy using optical microscope (OM), scanning electron microscope (SEM) and transmission electron microscope (TEM) at 120kV. In the case of non-homogenization, intermetallic compounds were observed, and rod-shaped precipitates were observed around intermetallic compounds. After homogenization at 848 K for 7.2 ks, the remaining intermetallic compounds, the platelets of equilibrium β phase and the rod-shaped precipitates were observed by OM observation. As a result of TEM observation, 2~3μm size of rod-shaped precipitates and cross-sections of the rod-shaped precipitates were observed for both the non-homogenization and the with-homogenization at 848 K for 7.2 ks. The SAED figures obtained from the side and cross sections of the rod-shaped precipitates were analyzed as β' phase. Optical microscopy showed that after hot extrusion of non-homogenization, a contrast was observed, suggesting that intermetallic compounds had been shattered by hot extrusion.

After hot extrusion of with-homogenization, a contrast of plate-like β-phase seen before hot extrusion and a contrast of plate-like β-phase possibly shattered by hot extrusion were observed.

Keywords: Homogenization, Al-Mg2Si, TEM, Extrusion, Precipitate

Email: †ikenolab@sus.u-toyama.ac.jp

P4-Spin switch effect of $TmFeO_3$ under low magnetic field

H. Song[1], S. X. Cao[1,2,‡]

[1]*Department of Physics, International Center of Quantum and Molecular Structures and Materials Genome Institute, Shanghai University, Shanghai 200444, China*

[2]*Shanghai Key Laboratory of High Temperature Superconductors, Shanghai University, Shanghai 200444, China*

Here we report the spin reorientation transition and spin switching of $TmFeO_3$, which crystallize in the distorted perovskite structure within the space group of *Pbnm*. Spin reorientation transition type of $TmFeO_3$ single crystal is Γ_4 (*Gx*, *Ay*, *Fz*) - Γ_2 (*Fx*, *Cy*, *Gz*), phase transition temperature range is 82-95 K. Under low magnetic field of 20 Oe, magnetization of *a*-axis suddenly drops at 80 K in field-cooled-warming (FCW) mode, namely, the type-II spin switch effect occurs. In the field-cooled-cooling (FCC) mode, magnetization suddenly jumps at 50 K, which is "reverse" type-II spin switch effect, and has not been reported. This interesting phenomenon is caused by the 180° reversal of the Tm^{3+} magnetic moment coupled with Fe^{3+} magnetic moment induced by magnetic field and Fe^{3+} crystal field. With the increase of magnetic field, the spin switching effect moves towards high temperature. When the external magnetic field increases to a certain value, the spin switching effect is completely suppressed. Meanwhile, type-II spin switch effect also happens along the *c*-axis.

Keywords: $TmFeO_3$, Spin reorientation transition, Spin switch effect

Email: ‡sxcao@shu.edu.cn

ICPMAT 2022 Shanghai 中国
16th International Conference on the Physical Properties and Application of Advanced Materials
21st-23rd November, 2022

P5-Hot electron extraction in SWCNT/TiO_2 for photocatalytic H_2 evolution from water

M. Yamagami[1], T. Tajima[1], H. K. Nguyen[2], K. Yashima[2], T. Matsubayashi[2], N. Nishiyama[2], T. Hayashi[2], Z. Zhang[3], J. Kano[3], Y. Takaguchi[2†]

1 Graduate School of Environmental and Life Science, Okayama University, Okayama 700-8530, Japan

2 Department of Material Design and Engineering, Faculty of Sustainable Design, University of Toyama, Toyama 930-8555, Japan

3 Graduate School of Natural Science and Technology, Okayama University, Okayama 700-8530, Japan

Single-walled carbon nanotubes (SWCNTs) have attracted attention for their application as a photoelectric conversion material due to their outstanding solar light absorption property. Recently, we found that water-dispersible coaxial nanowires with SWCNT/C_{60} heterojunctions prepared by the physical modification of SWCNTs with fullerodendrons exhibit photocatalytic H_2-production activity. However, C_{60} is not capable of extracting hot electrons from SWCNTs. On the other hand, Parkinson and co-workers fabricated SWCNT heterojunctions with atomically flat surface of TiO_2 and SnO_2, where higher-energy second excitonic SWCNT transitions produce more photocurrent. Because of the continuum of states within the metal-oxide conduction band with a density that increases with increasing energy above the conduction band minimum, rates of carrier injection from the second excited state (E_2 state) of SWCNT to TiO_2 or SnO_2 are competitive with fast hot-exciton relaxation processes. In this context, the construction of similar photocatalytic systems is of interest in order to make photocatalytic reactions using SWCNTs more efficient. In this paper, we synthesized SWCNT/TiO_2 nanohybrids to demonstrate their photocatalytic activity for hydrogen evolution from water through the hot electron extraction from the E_2 state of SWCNT to TiO_2.

Keywords: Single-walled carbon nanotubes, Photocatalyst, Hydrogen evolution

Email: pxua99lq@s.okayama-u.ac.jp

O6-Spin switching effect in $Nd_{0.8}Pr_{0.2}FeO_3$ single crystal

Z. Q. Sun[1], S. X. Cao[1,2‡]

[1]*Department of Physics, Materials Genome Institute and International Center for Quantum and Molecular Structures, Shanghai University, Shanghai 200444, China*

[2]*Shanghai Key Laboratory of High Temperature Superconductors, Shanghai University, Shanghai 200444, China*

The single crystal of $Nd_{0.8}Pr_{0.2}FeO_3$ was successfully grown by the optical floating zone method. Room temperature x-ray diffraction and Laue photograph declared the homogeneity and high quality of the single crystal. Magnetic measurements were characterized by using the 2.5 millimeters cubic sample of $Nd_{0.8}Pr_{0.2}FeO_3$ single crystal, which exhibit spin switching effects in two measurement modes of zero-field-cooling (ZFC) and field-cooling (FC) magnetization vs temperature (*M-T*) curves under different magnetic fields. Spin reorientation transition occurs near 74-110 K, where the spin configuration of the iron sublattice changes from Γ_4 to Γ_2. The type-I spin switching effect (i.e. magnetization drop) in ZFC mode has been reported in $NdFeO_3$ single crystals, but it has not been observed in FC mode in the parent materials of $NdFeO_3$ and $PrFeO_3$ single crystals. In other words, through the doping of Pr^{3+}, there is a new phenomenon in $Nd_{0.8}Pr_{0.2}FeO_3$ single crystal that has not been seen before in parent materials. As the temperature drops to 12 K, a new magnetic interaction mechanism works, which results in a further enhancement of magnetization.

Keywords: Rare-earth orthoferrite, Spin reorientation transition, Spin switching effect

Email: sxcao@shu.edu.cn

P7-Evaluation of electrochemical properties of batteries prepared by aerosol deposition method

N. Akiyama[1], T. Hashizume[2], A. Saiki[2]

[1]*Department of Material Science and Engineering, University of Toyama, Toyama, Japan*

[2] *School of Sustainable Design, a University of Toyama, Toyama, Japan*

All-solid-state batteries have the problem of high interface resistance. In all-solid-state batteries, powder materials are pressed together. As a result, the low packing density of the pressed powder is the cause of the electrical resistance. Sintering is one way to increase the packing density of the pellets. In this method, the cathode active material and solid electrolyte react during sintering, resulting in a high resistance layer. Therefore, it is necessary to create high-density layers without sintering. One method is the aerosol deposition (AD) method. The AD method is a film deposition method in which particles are accelerated by gas pressure, and the powders are impacted to the substrate at high speed to form layers. The AD method can produce dense films at room temperature. The objective of this study is to create and reduce the interface resistance of all-solid-state batteries using the AD method.

Cathode active material, oxide solid electrolyte, and anode active material were deposited on a copper plate in layers in sequence by the AD method. The electrochemical properties of the batteries were evaluated. The raw material and each layer of post-deposited were identified by XRD and microstructures were observed by SEM.

Keywords: Solid electrolyte, Battery characteristic, Lithium ion battery, Aerosol deposition method, Solid state battery

Email: saiki@sus.u-toyama.ac.jp

P8-Magnetodielectric effect and magnetoelectric coupling of $Co_3NiNb_2O_9$ single crystal

S. Zhu[1], C. F. Shi[1], G. Zhao[1], W. T. Yang[1], H. Y. Chen[1], X. X. Ma[1], J. Zhou[2], B. J. Kang[1,3], J. K. Bao[1,3*], S.X. Cao[1,3‡]

[1]*Department of Physics, Materials Genome Institute and International Center for Quantum and Molecular Structures, Shanghai University, Shanghai, 200444, China*

[2]*School of Physics and Electronic Engineering, Zhengzhou University of Light Industry, Zhengzhou, 450002, China*

[3]*Shanghai Key Laboratory of High Temperature Superconductors, Shanghai University, Shanghai, 200444, China*

High quality Ni-doped $Co_4Nb_2O_9$ single crystals of $Co_3NiNb_2O_9$ have been synthesized for using optical floating zone technique. In this paper, the structure, magnetic properties, magnetodielectric effect and magnetoelectric coupling of $Co_3NiNb_2O_9$ single crystals are investigated. The single crystal structure was determined by room temperature powder X-ray diffraction and Laue back-ray X-ray diffraction. Field-dependent magnetizations at 20 K along [100] and [120] directions have a slope change at 6 and 9 kOe, respectively, indicating a spin-flop transition or spin rotation in the *ab* plane. The temperature dependence of the dielectric constant and pyroelectric currents along [100] and [120] directions show a magnetic-field-induced peak near the antiferromagnetic transition temperature of T_N = 32 K, respectively, proving a sizable magnetodielectric effect and magnetoelectric coupling. With the increase of magnetic field, the electric polarization increases to 128 μC/m^2 along [120] axis under applied magnetic field of 40 kOe.

Keywords: Corundum-type Structure, Magnetodielectric Effect, Magnetoelectric Coupling

Email: ‡sxcao@shu.edu.cn, *jinke_bao@shu.edu.cn

P9-Growth of lithium niobate single crystals using the floating zone method and changes in physical properties due to Na addition

S. Kawara[1], T. Hashizume[2], A. Saiki[2]

[1]*Department of Material Science and Engineering, University of Toyama, Toyama, Japan*

[2]*School of Sustainable Design, University of Toyama, Toyama, Japan*

Piezoelectric are useful as actuator and sensor elements. Lead zirconate titanate (PZT) is a typical piezoelectric ceramic material. However, soil and marine contamination of lead is a issues. In this study, we focused on single crystals of lithium niobate because it is a ferroelectric material and environmentally friendly compared to PZT.

Single crystals were grown by using the Floating Zone Method (FZ method).Their piezoelectric properties were evaluated. The crystals grown were partly polycrystalline. The grown crystals were measured X-ray diffraction and elemental analysis. As a result, the grown crystal was confirmed to be a single crystal of lithium niobate. The admittance of the sample was measured using two-terminal method. The piezoelectric resonance was confirmed. From this, the piezoelectricity of the sample was checked. Single crystals were also grown adding a certain amount of sodium niobate. As a result, a change of physical property appeared in the analysis results compared to lithium niobate.

Keywords: Single crystal, Piezoelectric effect, Electronic components

Email: saiki@sus.u-toyama.ac.jp

P10-Flux Pinning Evolution of Pb Multilayer Thin Films in the purely repulsive interaction system

L. X. Gao[1], J. Y. Ge[1,2*]

[1]*Materials Genome Institute, Shanghai University, 200444 Shanghai, China*

[2]*Shanghai Key Laboratory for High Temperature Superconductors, Shanghai University, 200444 Shanghai, China*

Artificial Pb multilayer films were prepared to act as an alternative approach to study multicomponent superconducting systems. The additional repulsive length and the coupling strength among superconducting films were regulated by increasing the thickness of insulting films. The magnetization measurements were performed to clarify the effect of the competition between the repulsive vortex interactions on the macroscopic superconductivity of Pb multilayer films. The vortex phase diagram and the optimum critical current density have been determined. Furthermore, the second magnetization peak appears because the upper layer provides the weak pinning sites to localize the flux lines. The pinning behaviors switches to the mixed type with the increase of the insulting layer thicknesses. Our results open a new perspective to the study and related applications of the multilayer superconducting films.

Keywords: Multilayer superconducting film, Competing interaction, Flux pinning mechanism

Email: gaolixin@shu.edu.cn

P11-Mechanical properties and precipitation of Al-4mol%Zn-2mol%Mg-1mol%Cu alloy

Y. Sekiguchi[1], T. Tsuchiya[2], S. Lee[2], S. Ikeno[3], K. Matsuda[2†], K. Shibata[4], H. Matsui[4], T. Yoshida[4], S. Nishikawa[4], S. Murakami[4]

[1]Graduate School of Science and Engineering, University of Toyama, Toyama, Toyama, 930-8555, Japan

[2] Faculty of Sustainable Design, Department of Materials Design and Engineering, University of Toyama , Toyama, Toyama, 930-8555, Japan

[3]Professor emeritus, University of Toyama, Toyama, Japan

[4]AISIN KEIKINZOKU Co.,Ltd., Imizu, Toyama, 934-0031, Japan

7xxx series alloys (Al-Zn-Mg alloys) have a high strength compared to other Al alloys due to its good age hardenability. The precipitation sequence of this series alloy is known to be as follows:
S.S.S.S. → G.P.zone → η', T' → η, T

Conventionally, these alloys have been strengthened by dispersion of fine precipitation by aging treatment. These days, it is needed that higher strength materials for automobile part in response to the trend of lightweighting. Al-Zn-Mg alloys are good materials for satisfying the industrial needs. However, the limitation is clear, and it is needed stronger mechanical property. We have focused on the effect of Cu in Al-Zn-Mg alloy and reported better mechanical property with formation of fine precipitation. Also, we have reported that Zn/Mg=2 was shown the maximum hardness with aging treatment in Al-Zn-Mg alloys. Based on previous results, Cu and grain refiner (Zr, Ti) were added to the Zn/Mg=2 alloys and investigated age hardening behavior and mechanical properties in Al-Zn-Mg alloys.

The purpose of this study was to produce alloys with even higher strength and ductility and to investigate the effect of grain refiner. Two kinds of alloys were fabricated by casting of Al-4.0%Zn-2.0%Mg-1.0Cu alloy and Al-4.0%Zn-2.0%Mg-1.0Cu-Ti-Zr (in at.%) alloy. The alloys are denoted as ZM42HC and ZM42HCTZ, respectively. Homogenization treatment was conducted at 748K for 86.4ks, then samples were subjected to hot extrusion. Solution heat treatment was conducted at 748K for 3.6ks, and then quenched in cold water. Heat treatment was performed by changing the aging temperature using silicone oil bath. Micro-Vickers hardness was measured using Mitutoyo HM-101 (load: 0.98 N, holding time 15s). Tensile specimens were cut from extruded sheets with 0.8 mm×6.0 mm of cross-section and 17.5 mm of gauge length. The peak-aged samples at 393 K, and were fractured at room temperature using Instron type tensile machine. TEM (Topcon EM-002B) observation was conducted under the accelerated voltage of 120kV.

Keywords: Al-Zn-Mg, Grain refiner, TEM
Email: †ikenolab@sus.u-toyama.ac.jp

ICPMAT 2022 Shanghai 中国
16th International Conference on the Physical Properties and Application of Advanced Materials
21st-23rd November, 2022

P12-Crystal growth and physical properties evolution in $Ni_{1-x}Co_xTe_{2-\delta}$ system

W. B. Wu[1, ‡], Y. Q. Chen[1], L. X. Gao[1], L. Z. Zhang[1], Q. L. Xiao[1*], J. Y. Ge[1,2*]

1 *Materials Genome Institute, Shanghai University, Shanghai 200444, China.*

2 *Zhejiang Laboratory, Hangzhou, 311100, China.*

Transition metal tellurides have been widely studied for their diverse crystal structures and exotic physical properties such as large magnetoresistance, charge density waves, superconductivity, ferromagnetic, and topological properties. $NiTe_2$ has recently been found to be a Dirac semimetal, allowing it to achieve exotic properties by pressure and doping. We synthesize a series of $Ni_{1-x}Co_xTe_{2-\delta}$ single crystals by the standard solid-state reaction method. EDX and XRD tests confirm Co is successfully doped into the crystal structure. Normalized resistance of the samples shows metallic behavior. Magnetization measurements show that, in the doping range of $x = 0.12 \sim 0.62$, the samples exhibit coexistence of ferromagnetic and paramagnetic phases above the transition temperature T_t. By using the combined Curie–Weiss and Spin-wave model, the antiferromagnetic to ferromagnetic transition is found to occur as the temperature drops below Tt. The magnetic transition is attributed to the Te vacancies, which can be explained using the BMP model. A magnetic phase diagram for $Ni_{1-x}Co_xTe_{2-\delta}$ system is constructed.

Keywords: $Ni_{1-x}Co_xTe_{2-\delta}$ single crystals, Magnetic behavior, Antiferromagnetic to ferromagnetic transition

Email: wwweibin@shu.edu.cn

ICPMAT 2022 Shanghai 中国
16th International Conference on the Physical Properties and Application of Advanced Materials
21st-23rd November, 2022

P13-Superconductive Property of Nb_3Al/Al Composite Materials

S. Yamaguchi[1‡], K. Mastuda[1], T. Namiki[1], and K. Nishimura[1]

1 *Material Science and Engineering Major, Graduate School of Science and Engineering, Toyama University*

Several superconductors with the A15-type crystal structure have relatively high superconducting transition temperatures. Among them, Nb_3Sn has been widely used due to the high superconducting critical magnetic field. Nb_3Al has the same crystal structure, which is more resistant to strain/stress and has a higher critical field at its stoichiometric composition than Nb_3Sn. Although Nb_3Al has some superior superconducting properties, the manufacturing process is complex and the workability is poor. Thus, we fabricated Nb_3Al/Al composites by the three-dimensional permeation casting (3DPC) method to improve the workability. In this study, we prepared three samples using Nb_3Al particles and molten metal of pure Al or Al-10at%Si alloy, with different molten metal temperatures and cooling methods. The preparation conditions were, 1) molten Al at 800°C/air cooling, 2) molten Al at 800°C/quench in ice water, and 3) molten Al-10at%Si alloy at 650°C/quench in ice water. X-ray diffraction measurements of these samples showed that some of the Nb_3Al particles reacted with molten Al in all the samples, leading to the non-superconducting $NbAl_3$. SEM observations revealed, therefore, that the surfaces of the Nb_3Al particles were covered by the $NbAl_3$ layer. The magnetization and electrical resistivity measurements indicated the noticeable superconducting transition signals with each sample, but the diamagnetic signal of the superconducting transition is far smaller than the ideal value, and the electrical resistivity did not reach zero below the transition.

Keywords: Superconductor, Nb_3Al, 3DPC

Email: ‡m2171530.ems@u-toyama.ac.jp

P14-The effect of granularity on superconducting properties of Pb films

J. Y. He[1], H. F. Qin, Q. L. Xiao, J. Y. Ge[1,*]

[1]*Materials Genome Institute, Shanghai University, Shanghai 200444, People's Republic of China*

In our research, the superconducting Pb films with different grain sizes and morphology were prepared by using low temperature electron beam evaporation technique on various substrates. With decreasing grain size, the upper critical field of Pb films increases and Pb films are prone to feature flux avalanche at low magnetic fields in the M - H curves. Further analysis suggests that with decreasing grain size the pinning mechanism evolves from a mixed δl to the δTc pinning mechanism. Our results open a new perspective to the study of pinning mechanism for granular superconductors and is beneficial to the potential application of manipulating vortex pinning by adjusting the granularity of superconducting films

Keywords: The superconducting Pb films, Different substrates, Flux avalanche, Pinning mechanism

Email: 1035605141@shu.edu.cn

P15-DSC analysis and TEM microstructure observation of Al-1.0Mg_2Ge alloy

S. Ukita[1], S. Murakata[1], T. Tsuchiya[2], S. Lee[2], S. Ikeno[3], and K. Matsuda[2, †]

[1]Graduate School of Science and Engineering, University of Toyama, Toyama, Toyama, 930-8555, Japan

[2] Faculty of Sustainable Design, Department of Materials Design and Engineering, University of Toyama , Toyama, Toyama, 930-8555, Japan

[3]Professor emeritus, University of Toyama, Toyama, Japan

Al-Mg-Ge alloys, as well as Al-Mg-Si alloy, are treated as Al-Mg2Ge pseudo-binary type alloys and have been researched to analyze aging precipitation of Al-Mg-Si alloys. There are several reports on the aging precipitation process of Al-Mg-Ge alloys, and it is basically the same as that of Al-Mg-Si alloys, i.e., supersaturated solid solution → G.P. zone → β' phase → β phase (Mg2Ge).However, it has been reported that Al-Mg-Ge alloys have a unique aging precipitation process in which clusters are formed in a higher density and are less likely to grow compared to Al-Mg-Si alloys. It was also reported that type-A precipitates formed in Al-Mg-Si alloys of excess Si type were also observed in Al-1.0 mass%Mg2Ge alloys of balanced composition, but the aging phenomenon was not fully clarified. Therefore, the purpose of this study is to understand the behavior of aging precipitation of Al-Mg-Ge alloy from the initial stage of precipitation using differential calorimetry (DSC), Vickers microhardness tester and high-resolution transmission electron microscopy (HR-TEM). DSC measurements performed at heating rate of 10℃/min and a temperature range of 25 to 500℃. DSC measurements stopped at aimed temperature and cooled down to room temperature. Then, samples were conducted hardness measurement and prepared TEM samples. Microstructure observation was carried out using HR-TEM(Topcon EM-002B) under accelerate voltage of 120kV.

Keywords: Al-Mg-Ge, Precipitate, TEM

Email: †ikenolab@sus.u-toyama.ac.jp

P16-Yttrium and Praseodymium doped proton conducting electrolytes with improved sinterability.

T. Miyazono[1], T. Hashizume[2], A. Saiki[2]

[1]*Department of Material Science and Engineering, University of Toyama, Toyama, Japan*

[2]*School of Sustainable Design, a University of Toyama, Toyama, Japan*

Proton conductors are widely used in hydrogen sensors and fuel cells. Hydrogen sensors and fuel cells in which the proton conductor barium zirconate is used are clean energy materials. Barium zirconate is chemically stable. Barium zirconate powder is industrially sintered at high temperatures, but at that time volatilization of barium during sintering is a problem. In this research Barium zirconate doped with praseodymium (Pr) and yttrium (Y) can improve sinterability issues and improving the proton conductivity. We investigated the effect of concentration dopants on the sintering behavior and oxygen defects of the proton-conducting electrolyte materials by varying the concentration of Pr and Zirconium (Zr) at the 'B' site of the perovskite structure ($BaZr_{0.70}Y_{0.20}Pr_{0.10}O_{3-\delta}$, $BaZr_{0.75}Y_{0.20}Pr_{0.05}O_{3-\delta'}$, $BaZr_{0.80}Y_{0.20}O_{3-\delta''}$) while keeping the concentration of Y constant. The Pr doping successfully improved the sinterability even at the temperature of 1450 ℃. The increase in the concentration of Pr improved the proton conductivity by 10^{-2} S/cm^2 at the temperature of 150℃.

Keywords: Barium zirconate, Sinterability, perovskite, Proton-conducting

Email: ‡saiki@sus.u-toyama.ac.jp

P17-Superconducting state properties of Cu-doped $NbTe_2$ single crystals

J. F. Chen[1,2,3], Z. J. Feng[1,2,3,4‡]

[1]*Materials Genome Institute, Shanghai University, Shanghai, 200444, China*

[2]*Zhejiang Laboratory, Hangzhou 311100, China*

[3]*Shanghai Laue Sci. & Tech. Institute, Shanghai, 200444, China*

[4]*Shanghai Key Laboratory of High Temperature Superconductors, Department of Physics, Shanghai University, Shanghai, 200444, China*

$NbTe_2$ is a monoclinic quasi-two-dimensional layered semimetal. This paper reports the change of physical properties of NbTe2 single crystals under the action of copper substitution. We found that doping Cu can enhance the superconductivity of Nb1-x(Cux)Te2 single crystal samples, increasing the superconducting transition temperature from 0.5 K to 3 K. As the doping concentration of Cu element increases to x=0.1, the superconducting transition temperature disappears. The zero-field ab-surface resistivity ρxx shows that the sample is metal. Magnetoresistance changes of up to 23% were observed at a magnetic field of 13 T without any tendency to saturate, and linear magnetoresistance was observed at high magnetic fields. The curve of the Hall resistance changing with the magnetic field at the same temperature has a linear relationship with the magnetic field, and the slope is positive, indicating that the carrier type is mainly hole-type carriers. These results suggest that Superconductivity of Nb1-x(Cux)Te2 enhanced by Doping Cu may provide a new platform for our understanding of superconductivity in transition metal dichalcogenides.

Keywords: Electronic structure, superconductor, transition metal dichalcogenides

Email: fengzhenjie@shu.edu.cn

ICPMAT 2022 Shanghai 中国
16th International Conference on the Physical Properties and Application of Advanced Materials
21st-23rd November, 2022

P18-Effect of injection molding conditions of carbon fiber reinforced PEKEKK resin on retainer

K. Yabashi[1], T. Isezaki[1], T. Tsukeda[2], T. Aida[2], Y. Funato[3], and S. Kajikawa[4]

[1]*University of Toyama, Graduate School of Science and Engineering, Toyama, 930-8555, Japan*

[2]*University of Toyama, Faculty of Sustainable Design, Toyama, 930-8555, Japan*

[3]*TC Toyama Co., Ltd., Toyama, 930-0274, Japan*

[4]*Makino Milling Machine Co., Ltd., Advanced Technology Section, Kanagawa, 243-0303, Japan*

In recent years, fuel efficiency improvement in the transportation equipment field, such as aircraft and automobiles, has become an issue due to the reduction of carbon dioxide emissions for global warming control and unstable oil prices. Carbon fiber-reinforced plastics, which are made by mixing carbon fibers and plastics, have excellent specific strength and specific rigidity, and are now widely used in aircraft, automobiles, ships, and other transportation equipment, as well as in machine tools. In addition, as various types of equipment become smaller, lighter, and more efficient, the development of engineering plastics with high performance and multifunctionality has been remarkable, and the operating environment temperatures of plastic parts using these plastics have become increasingly hotter. In machine tool spindles, the development of machining centers since 1975 has led to a rapid increase in demand for higher speeds to improve cutting efficiency, and the development has focused on high-speed technology. As spindle speeds increase, new materials must be applied to bearings (rolling elements, inner/outer rings, and retainer), and design methods and analysis techniques must become more sophisticated.

In this study, we focused on poly-ether-ketone-ether-ketone-ketone (PEKEKK) resin, which has even better heat resistance than that of poly-ether-ether-ketone (PEEK), thermoplastic material with excellent performance among heat-resistant resins. PEKEKK resin has excellent heat resistance characteristics, however, requires high melting temperatures during injection molding. It has also been found that adding carbon fiber to the base resin material can improve its mechanical properties. PEKEKK resin was used as the base material, and a mixed material with 30 wt% carbon fiber added as reinforcement was used as the test material. The retainer was injection molded using a pre-plunger type machine as the molding method.

Injection molding conditions were set at a resin temperature of 420°C, an injection speed of 75 mm/s, and a holding pressure of 420 MPa. The position at which the injection process is switched to the holding pressure process (holding pressure switching position) was varied during the molding process. The influence of injection molding conditions on the retainer at that time was evaluated using roundness, as well as weight, tensile test, DSC, etc., to study the optimal injection molding conditions.

Keywords: PEKEKK, Carbon fiber, Injection molding, Roundness

Email: s1890260@gmail.com

P19-Microstructure and microwave absorption properties of FeCoNiCuGe high-entropy alloys

Y. F. Zhang[1,2,3], J. Y. He[1,2], J. F. Chen[1,2,3], Y. H. Chen[1,2,3], and Z. J. Feng[1,2,3,4,†]

[1]*Materials Genome Institute, Shanghai University, Shanghai 200444, People's Republic of China*

[2]*Zhejiang Laboratory, Hangzhou 311100, China*

[3]*Shanghai Laue Sci. & Tech. Institute, Shanghai, 200444, China*

[4]*Shanghai Key Laboratory of High Temperature Superconductors, Department of Physics, Shanghai University, Shanghai, 200444, China*

Owing to the development of electronic information technology, electromagnetic (EM) wave has been widely used in many fields, such as information communication, biomedical, military action. However, the following problem, EM pollution, has been increasingly extrusive. EM wave absorption materials possessing exceptionally high EM energy loss efficiency has attracted many researchers' attention. High-entropy alloys (HEAs) possess complex structural and magnetic properties due to those multi-element phases and lattice distortion. Phase evolution, annealing behaviors, microstructure, magnetic and EM wave absorption properties of FeCoNiCuGe HEAs powders synthesized by mechanical alloying are investigated. The microstructure and EM wave absorption properties of HEAs powders after high-energy planetary ball milling for different time (1 h, 10 h, 30 h, 50 h, 70 h) and different annealing temperature (623 K ,723 K, 823 K) are compared. This work provides precious and insightful information for introducing high-entropy soft magnetic alloys to improve the properties of EM wave absorption materials applied in increasingly severe environments.

Keywords: Microstructure, Microwave absorption, High-entropy alloys

Email: ‡fengzhenjie@shu.edu.cn

ICPMAT 2022 Shanghai 中国
16th International Conference on the Physical Properties and Application of Advanced Materials
21st-23rd November, 2022

P20-Investigation of manufacturing conditions of single roll rapidly solidified ribbon for anode materials of Mg rechargeable batteries by using thermal-hydraulics CAE

Y. Kirimoto[1], T. Tsukeda[2], T. Aida[2], Y. Nemoto[3], M. Ikeda[4], H. Tabata[4], H. Kurihara[5], M. Suzuki[6]
[1]*University of Toyama, Graduate School of Science and Engineering, Toyama, 930-8555, Japan*
[2]*University of Toyama, Faculty of Sustainable Design, Toyama, 930-8555, Japan*
[3]*Flow Science Japan, Inc. Engineering Department Senior Sales Engineer, Tokyo, 111-0041, Japan*
[4]*Chuetsu Metal Works Co., Ltd., Advanced Technology Laboratory, Toyama, 930-0298, Japan*
[5]*Saitama Industrial Technology Center (SAITEC), Saitama, 333-0844, Japan*
[6]*Toyama Prefectural University, Faculty of Engineering, Toyama, 939-0398, Japan*

In recent years, the social implementation of rechargeable batteries used for the electrification of transportation equipment and renewable energy has become an issue to meet sustainable development goals, and the development of innovative rechargeable batteries is required. Magnesium rechargeable batteries are attracting attention as next-generation rechargeable batteries because of their resource abundance, cost, safety, and high electrical capacity per volume compared to conventional lithium-ion rechargeable batteries.

Our joint research team focused not only on the electrochemically active magnesium composition of ribbon for the negative electrode materials of magnesium rechargeable batteries, but also on the production process, focused on the single roll type liquid quenching and rapid solidification method, which can be produced at a lower cost. The single roll method is a mass production technology in which molten metal is rapidly cooled and solidified on the outer circumference of a high-speed rotating roll to continuously produce metal ribbons in a single process. Not only does it have the advantages of high productivity and easier equipment compared to twin rolls and rolling in terms of production technology, but it is also suitable for magnesium alloys that have low plastic workability at room temperature due to their crystalline structure.

The technical key to the single roll method is to make the nozzle opening that spurts out molten metal slit-shaped and to keep the distance between the nozzle and the rolls close to an appropriate distance. By keeping the nozzle and rolls close together, surface tension acts on the molten metal to form a puddle. The major control factors in the single roll method are the nozzle slit size, jetting pressure, roll peripheral speed, nozzle-to-roll distance, and molten metal temperature, which govern the thickness, width, and surface properties of the ribbon.

In this study, the optimal processing conditions were examined by comparing CAE analysis with ribbon actually manufactured, with the aim of further improving manufacturing conditions using the same method, such as length discontinuities, thickness, and surface properties of ribbon. The CAE analysis

software used was Flow3D®, a thermal flow CAE software manufactured by Flow Science, Inc. We specifically various process parameters such as injection pressure and roll peripheral speed for evaluation.

Keywords: Mg rechargeable batteries, Single roll rapidly solidified, Thermal-hydraulics CAE

Email: d2272101@ems.u-toyama.ac.jp

ICPMAT 2022 Shanghai 中国
16th International Conference on the Physical Properties and Application of Advanced Materials
21st-23rd November, 2022

P21-Magnetic phase transitions and giant magnetic coercivity in $Mn_{2.45}Fe_{0.58}Sn_{0.97}$ single crystals

W. H. Shen[1], Y. L. Huang[2], X. Y. Yao[3], F. Y. Qi[4], G. X. Cao[*]

[1]*Materials Genome Institute, Shanghai University, Shanghai, 200444, China*

The magnetic transition and transport properties of the $Mn_{2.45}Fe_{0.58}Sn_{0.97}$ single crystals with a hexagonal structure have been investigated. This noncollinear antiferromagnetic single crystal exhibits a Neel temperature of 297 K. After cooling from 297 K, a magnetic phase transition from noncollinear antiferromagnetism to ferromagnetism occurs at 200 K due to the tilting of magnetization towards c axis. Below this temperature, a topological Hall effect (THE) starts to appear due to the non-vanishing scalar spin chirality arising from the noncoplanar spin structure. Interestingly, the topological Hall resistivity is found to be as high as about 4 μΩ cm at 100 K in the xy-plane (0001). When the applied magnetic field is parallel to the c-axis, another magnetic transition occurs at 187 K, resulting in the coexistence of ferromagnetism and antiferromagnetism at low temperature. Therefore, a giant coercivity up to about 30 kOe is obtained at 2 K due to the pinning effect of antiferromagnetism on the ferromagnetic phase. However, when the external magnetic field is perpendicular to the c-axis, the magnetization curve has almost no hysteresis. Therefore, the material is easily magnetized perpendicularly and has broad application prospects in the field of perpendicular magnetic recording.

Keywords: magnetic transition, non-collinear antiferromagnet, topological Hall effect

Email: guixincao@shu.edu.cn

P22-Effect of process parameters on anode activity of Mg-6%Al-3%Ca alloy ribbons manufactured by single-roll atmospheric rapid solidification method for Mg rechargeable batteries

K. Fuke[1], T. Tsukeda[1], T. Aida[1], M. Ikeda[2], H. Tabata[2], H. Kurihara[3], M. Suzuki[4]

[1]*University of Toyama, Toyama, 930-8555, Japan*

[2]*Chuetsu Metal Works Co., Ltd., Toyama, 930-0298, Japan*

[3]*Saitama Industrial Technology Center, Saitama, 333-0844, Japan*

[4]*Toyama Prefectural University, Toyama, 939-0398, Japan*

In recent years, lithium-ion batteries have been used in various devices such as information mobile devices and electric vehicles, but the uneven distribution of resources, the safety of components, and the limitations of high capacity require the development of new rechargeable batteries. High energy density is necessary for the development of next-generation rechargeable batteries, and Mg, Ca, Al, and other low-cost multivalent metals with high Clark's number are promising as anode materials from the viewpoint of securing resources and reducing costs. In particular, it has been reported that magnesium (Mg) rechargeable batteries do not precipitate in dendrite form when charged using Mg metal, which is easy to handle, as the negative electrode, enabling batteries with metal negative electrodes that are free from concerns about short circuits and ignition.

In this study, a composition of Mg-6mass%Al-3mass%Ca was selected (hereinafter referred to as AX63), and the anode material was fabricated by the rapid solidification method without using a vacuum chamber and vacuum exhaust system. We aimed to establish atmospheric manufacturing conditions for the purpose of reducing production costs and producing sound ribbons.

Specimen AX63 was made by casting high-purity Mg (99.9%), high-purity Al (99.9%), and Mg-Ca mother alloy, weighing them to obtain the target composition. After homogenization treatment in an electric furnace at 420℃ for 20 h and surface cutting, the material was processed using a 400ton vertical hydraulic press at an extrusion temperature of 350℃, an extrusion ratio of 7.06, and a ram speed of 1 mm/s. The billets were made into 19 mm diameters. billets and used as melting raw material for rapid cooling and solidification. In the single roll type rapid cooling and solidification apparatus, an oxygen-free copper cooling roll of 20 mm in width and 200 mm in diameter without cooling water was used. A cut raw material billet of φ19 mm × 10 mm was inserted into a crucible with a 10 mm wide nozzle made of SUS430, heated and melted by a high frequency coil, and injected with Ar gas onto a high-speed rotating roll to produce a ribbon.

The production conditions were air atmosphere, injection pressure of 0.05 MPa, injection temperature fixed at 757℃ to achieve a superheat of 150℃, distance between nozzle and cooling roll, and peripheral

speed of cooling roll were varied to evaluate ribbons under a total of 9 conditions. The electrochemical activity of AX63 ribbon was evaluated by constant-current charge-discharge tests. In the observation of surface properties, the length and weight of ribbon samples made under each condition were measured, and the appearance of the front and back surfaces were photographed to evaluate soundness at the visual level. The thickness of the ribbon was measured using a digital microscope after each ribbon specimen was embedded in cold-impregnated resin. Ten cross sections of ribbon were measured and the average value was obtained. Identification of the crystalline phases were performed using XRD. The orientation of each ribbon was also evaluated based on XRD measurements.

Keywords: Mg-Al-Ca alloy, Rechargeable batteries, Single-roll atmospheric rapid solidification method
Email: kousukedenden@gmail.com

P23-High-throughput X-ray characterization of discrete component samples of rare earth-doped thermal barrier coating materials

G. Wu[1], X. M. Song[2], Y. F. Zhang[1], Y. Zeng[2], Z. J. Feng[1,‡]

[1]*Materials Genome Institute, Shanghai University, Shanghai 200444, China*

[2]*Analysis and Testing Center for Inorganic Materials, Shanghai Institute of Ceramics, Chinese Academy of Sciences, Shanghai 200050, China*

With the continuous investment of researchers in the research and development of materials science, the high-throughput X-ray characterization technology is widely used in the process of material research and development, which greatly improves the research and development efficiency of new materials and is also an important tool for material genome engineering research. In this paper, a high-throughput X-ray characterization system is designed, and the X-ray source can perform high-precision X-Y two-dimensional plane translation, and under the condition of ensuring the quality of the data sample, multiple discrete samples can be detected in a very short time, and the influence of different content of rare earth element doped thermal barrier coating materials on their structural phase stability is explored.

Keywords: High-throughput X-ray characterization, Thermal barrier coating, Rare earth elements

Email: ‡ fengzhenjie@shu.edu.cn

ICPMAT 2022 Shanghai 中国
16th International Conference on the Physical Properties and Application of Advanced Materials
21st-23rd November, 2022

P24-Effect of Ag Addition on Corrosion Properties of Mg-Al Alloys

G. Ota[2], K. Sarayama[1], K. Nakano[1], Y. Simada, [1] A. Morihiro [2], M. Hatakeyama[3], S. Sunada[3], K. Sato[4]

1*Graduate School of Material Science and Engineering for Education, University of Toyama, 3190 Gohuku Toyama, 930-8555, Japan*

2*Undergraduate Student of Department of Materials Design and Engineering, University of Toyama, 3190 Gohuku Toyama, 930-8555, Japan*

3*Graduate School Material of Science and Engineering for Research, University of Toyama, 3190 Gohuku Toyama, 930-8555, Japan*

4*Graduate School of Science and Engineering, Kagoshima University, Korimoto Kagoshima 890-0065, Japan*

In the Ag added Mg-Al alloys, Miao et al. reported that Ag is unevenly segregated at the α-β interfaces and in β phase. [1] Corrosion properties in such cases are not understood. In order to investigated corrosion behavior of α and β phase in the Mg-Al-Ag alloys, Mg-9Al (AM90), Mg-9Al-0.5Ag (AQ905), Mg-43Al (β single phase), and Mg-43Al-2Ag (β-2Ag phase) were prepared for the electrochemical measurements. Structural studies of β phases are carried out using X-ray diffraction (XRD). Electron probe microanalysis (EPMA) was used to measure the distributions of Ag in the AQ905. Anodic polarization curve measurements were performed in all samples. The corrosion potential of the β-2Ag was higher than that of the β single-phase because of the higher standard potential of Ag (E_0 = +0.8 V), which has a higher standard potential than that of the β phase. In AM90 and AQ905, the addition of Ag causes changes in corrosion potential and corrosion current density. Details of these results will be discussed in the conference.

Keywords: Magnesium alloy, Corrosion, Polarization test,

Email: ‡ s1990203@ems.u-toyama.ac.jp

P25-Stress corrosion behavior of friction stir welding joint of 7N01 aluminum alloy

Y. Z. Pan[1], S. W. Duan[2], F. Guo[1], K. Matsuda[3], T. Wang[1], Y. Zou[4]

[1]*Key Laboratory for Liquid-Solid Structural Evolution and Processing of Materials, School of Materials Science and Engineering, Shandong University, Jinan, 250061, China*
[2]*College of Nuclear Equipment and Nuclear Engineering, Yantai University, Yantai 264005, China*
[3]*Department of Materials Design and Engineering, Faculty of Sustainable Design, University of Toyama, Toyama 930-8555, Japan*
[4]*Shandong Engineering & Technology Research Center for Modern Welding, Shandong University, Jinan, 250061, China*

The friction stir welding joint of 7N01 aluminum alloy has strong stress corrosion sensitivity due to the inhomogeneity of microstructure. In this paper, the stress corrosion behavior of 14 mm thick plate 7N01-T4 welding joint and base metal was investigated by means of electrochemical impedance spectroscopy, slow strain rate tensile test and electron back scattered diffraction. The results show that the charge transfer resistance of the welding joint is obviously lower than that of the base metal. The lowest impedance at the joint is 698 Ωcm^2, but the lowest impedance is 1082 Ωcm^2 at the base metal.The lowest Rct value at the weld is only 64.5% of the base metal. The thermal-mechanical affected zone on the rear side is the worst area of the resistance to stress corrosion. There are more deformed grains and larger Schmidt factor close to 0.5 in this area, and the different grain orientation can easily lead to the concentration of internal tensile stress and the formation of crack propagation.

Keywords: 7N01 aluminum alloy; Friction stir welding joint; Stress corrosion; Slow strain rate tensile;
E-mail: panyz@mail.sdu.edu.cn

P26-B substitution effect on magnetic properties of $HoAl_2$

T. Fujimoto[1]‡, T. Namiki [1], and K. Nishimura[1]

[1]*Material Science and Engineering Major, Graduate School of Science and Engineering, Toyama University*

In recent years, magnetic refrigeration using magnetic materials has been widely studied as an efficient cooling method for hydrogen liquefaction. Among them, the HoB2 with the Curie temperature (TC) of 15 K has been found to exhibit the large magnetic entropy change |ΔSM(μ0H:5 T→0 T)| of 40.1 J kg K−1 near TC.[1] Previous studies have reported that Al substitution in HoB2 causes a separation into two phases, HoB2 and HoAl2, and an increase in the transition temperature of HoAl2.[2] This has been attributed to an increase in the volume of HoAl2 due to the intrusion of B atoms into HoAl2. Therefore, we investigated the effect of B-substitution in HoAl2 (HoAl2-xBx, x = 0, 0.1, 0.2, 0.3, 0.4, 0.5). The samples were prepared by an arc-melting process in an Ar atmosphere. From the magnetisation measurements, two ferromagnetic transitions at 30 K (TC1) and 16 K (TC2) were observed for samples above x = 0.2. The observed TC1 and TC2 little changed regardless of the amount of B. It was observed that the volume fraction of HoB2 increased as the amount of B increased.

Keywords: Magnetocaloric effect, B substitution, $HoAl_2$

Email: ‡m2171524.ems@u-toyama.ac.jp

ICPMAT 2022 Shanghai 中国
16th International Conference on the Physical Properties and Application of Advanced Materials
21st-23rd November, 2022

P27-Optimization of the mechanical properties of SAC105-based solder alloys via machine learning

S. T. Yu[1], K. D. You[1], B. Cao[1], Z. Q. Dong[1*], J. C. Zhang[1], T. Y. Zhang[1]

[1]*Materials Genome Institute, Shanghai University, Shanghai 200444, People's Republic of China*

The rapid development of electronic technologies imposes higher requirements on interconnect materials. Sn-Ag-Cu(SAC) based lead-free solder alloy is one of the major class interconnecting materials used in electronic industries. Tremendous efforts have been devoted to improving the properties of SAC solder alloys. Adding alloying elements is one effective approach. In the current study, the mechanical properties of SAC105 based solder alloys were optimized by using an Bayesian optimization strategy based machine learning approach. The strategy uses the upper confidence boundary function to balance the exploration and exploitation tradeoff for searching of the alloys with the enhanced properties. Meanwhile, a unified target function composed of the two conflicted properties (tensile strength and ductility) was defined for directing the solder alloy design. After three rounds iteration design loops integrated with the experimental validation, solder alloys which exhibit the evident improved mechanical properties were obtained. The designed new SAC105 based solder alloy demonstrates an outstanding mechanical property, yielding a significant improvement in tensile strength (35% improvement vs. SAC105) with an acceptable ductility (>20 %). The experimental results show a good agreement with the ML forecasts, demonstrating that ML is a powerful tool for designing lead-free solder alloys with optimized mechanical properties.

Keywords**:** Lead-free solder; Machine learning; Mechanical properties.

Email: * zqdong@shu.edu.cn

ICPMAT 2022 Shanghai 中国
16th International Conference on the Physical Properties and Application of Advanced Materials
21st-23rd November, 2022

P28-$MoSe_2$-sensitized water splitting assisted by C_{60}-dendron on the basal surface

H. K. Nguyen[1], T. Matsuura[2], T. Tajima[2], M. Yamagami[1], K. Yashima[1], T. Matsubayashi[1], N. Nishiyama[1], T. Hayashi[1], Y. Takaguchi[1,*]

1 *Department of Material Design and Engineering, Faculty of Sustainable Design, University of Toyama, Toyama 930-8555, Japan*

2 *Graduate School of Environmental and Life Science, Okayama University, Okayama 700-8530, Japan*

Transition metal dichalcogenides (TMDs) have attracted much attention because of their unique two-dimensional nanostructure and outstanding properties. Although there are many reports on the hydrogen evolution reaction (HER) using TMDs as an electrocatalyst or a co-catalyst, clear-cut examples of HER photosensitized by TMDs are quite rare. Herein, we prepared water-dispersible $MoSe_2$/fullerodendron nanohybrids by the physical modification of the basal surface of $MoSe_2$ using fullerodendron to explore its photosensitizing activity for HER from water. Their 2D/0D mixed-dimensional heterojunction ($MoSe_2/C_{60}$) is expected to generate a charge-separated (CS) state via photoinduced electron transfer from $MoSe_2$ to C_{60}. Fortunately, we observed efficient HER (70 μmol/h) from water using $MoSe_2$/fullerodendron nanohybrids in the presence of methyl viologen (MV^{2+}), Pt-nanoparticle, and 1-benzyl-1,4-dihydronicotinamide (BNAH). Action spectra for this HER clearly show $MoSe_2$ acts as not a co-catalyst but a photosensitizer in this reaction system. Then, upon photoexcitation of $MoSe_2$ by 800-nm-illumination, we observed a steady generation of hydrogen (1.1 μmol/h), of which external quantum yield (EQY) was 0.0027%.

Keywords: $MoSe_2$, C_{60}, Mixed-dimensional heterojunction, H_2 evolution, Photocatalyst, Water splitting

Email: m22c1625@ems.u-toyama.ac.jp

P29-Magnetic properties of Al-4%Cu(-Mn, -Fe) alloy

E. Hida[1,‡], T. Namiki[1], and K. Nishimura[1]

[1]*Material Science and Engineering Major, Graduate School of Science and Engineering, Toyama University*

In this study, the effect of transition metal additives on the precipitate microstructure of Al-Cu alloys was investigated via x-ray diffraction and magnetization measurements. We focused on the magnetic elements, Mn and Fe, which are often contained as impurities in aluminum alloys. Samples of Al - 4 % Cu – x % Mn (x = 0.5 , 1 , 2 , 3 , 4 , 5) and Al – 4 % Cu – y % Fe (y = 0.5 , 1 , 2 , 3 , 4 , 5) (at. %) were prepared by arc melting. Magnetization measurements were performed in the temperature range from 10 to 300K and in an external magnetic field of 7 T. Temperature dependences of the magnetization show that in the Al-Cu-Mn alloys magnetization increased with increasing the Mn concentration, while little change was observed among the Al-Cu-Fe alloys. On the XRD patterns of the Al-Cu-Fe alloys, nonmagnetic Fe compound, Al_7Cu_2Fe, was found. Contrarily, X-ray diffraction measurements showed few peaks of Mn or Mn compounds in the Al-Cu-Mn alloys. Thus, the solute Mn ions were considered to be solidly dissolved. Additionally, magnetic properties of single-phase Al_7Cu_2Fe, $Al_{13}Fe_4$, Al_6Mn, Al_2Cu, and Al_4Cu_9 compounds were examined.

Keywords: magnetic properties, Al-Cu-Mn alloy, Al-Cu-Fe alloy

Email: ‡m2171522@ems.u-toyama.ac.jp

P30-Magnetocaloric properties of $Ho_{1-x}Gd_xB_2$

S. Yosinaga[1,‡], T. Namiki [1], K. Nishimura [1]
[1]*Grad. Sch. of Sci. and Eng. for Edu., Univ. of Toyama*

HoB_2 has shown a very large magnetic entropy change ($|\Delta S_M|$) of 40.1 (J kg^{-1} K^{-1}) in a magnetic field change of 5 T near the ferromagnetic transition temperature (T_C = 15 K) near the boiling point of hydrogen [1]. This finding makes HoB_2 a good candidate for a magnetic refrigeration material to liquefy hydrogen gas. Substitution of Ho with Dy ($Ho_{1-x}Dy_xB_2$) decreased $|\Delta S_M|$, but increased T_C [2]. In this study, we report the effect of Gd substitution on the magnetocaloric properties of HoB_2. Since the de Gennes factor of Gd is larger than that of Dy, $Ho_{1-x}Gd_xB_2$ is expected to increase T_C with increasing x. The samples were prepared by arc melting method. Powder X-ray diffraction results show that the main phase is an AlB_2-type structure (P6/mmm). Then, magnetization and specific heat measurements were performed. From the magnetization measurements, T_C were evaluated to reach 17, 20, 22, and 26 K at x = 0, 0.1, 0.2, and 0.3, respectively. The obtained $|\Delta S_M|$ values of 31, 27, 27, and 21 J kg^{-1} K^{-1} at x = 0, 0.1, 0.2, and 0.3, respectively, using Maxwell's relation. The Relative Cooling Power (RCP) obtained by the product of $|\Delta S_M^{MAX}|$ and the width at half maximum (ΔT_{FWMH}) were 5.8, 5.8, 6.5, and 6.2 J kg^{-1} at x = 0, 0.1, 0.2, and 0.3, respectively. The decrease in $|\Delta S_M^{MAX}|$ and the increase in ΔT_{FWMH} with increasing in x resulted in the almost unchanged RCP. $Ho_{1-x}Gd_xB_2$ was found to have excellent magnetocaloric properties at high temperatures.

[1] Pedro Baptista de Castro et al., *NPG Asia Mater.,* 12, 35 (2020)
[2] Pedro Baptista de Castro et al., *Sci. Technol. Adv. Mater.,* 21, 849 (2020)

Keywords: magnetocaloric effect, substitution, HoB_2
Email: ‡m2171532@ems.u-toyama.ac.jp

P31-Superconductivity of La (111)/Si (100) thin films

C. Y. Wu[1], Y. Z. Wang[1], R. H. Ma[1], J. Han[1], J. Wang[1], F. Chen[1,*]

[1]*Materials Genome Institute, Shanghai University, Shanghai 200444, People's Republic of China*

As one of the rare-earth elements, lanthanum and its compounds, such as LaB6 and LaH10, exhibit unique physical and chemical properties, which have attracted lots of interests. Here we synthesize La epitaxial films on Si (100) substrate by molecular beam epitaxy (MBE) method. The corresponding XRD analysis suggests that the La films exhibits fcc crystal structure (β-La) with the (111) orientation. Magnetic measurements indicate that the onset superconducting transition temperature is about 5.4 K. A clear signature of the second magnetization peak (SMP) is observed in the isothermal magnetization curves. We calculated the critical current density (Jc), which is greater than 10 MA/cm2 when T < 4 K. Our results on La thin films may help to further understand the mechanisms of the second magnetization peak.

Keywords: La film, Superconductor, Second magnetization peak (SMP)

Email: chf001@t.shu.edu.cn

P32-Effect of rare earth addition on sodium tantalate prepared by solution process

Y. Arata[1], T. Hashizume[2], A. Saiki[2]

[1]*Department of Material Science and Engineering, University of Toyama, Toyama, Japan*

[2]*School of Sustainable Design, University of Toyama, Toyama, Japan*

One performance of photocatalysts is the production of hydrogen and oxygen when fine semiconductor powders are dispersed in water and irradiated by light. Sodium tantalate is another photocatalytic material. The addition of a few mol% of rare earth elements to sodium tantalate increases the speed of hydrogen production.

In this study, the effect of the crystal structure of sodium tantalate on the addition of rare earth elements was investigated. 3 types of sodium tantalate powders (La, and Sm or non-doped) were prepared by hydrothermal synthesis. The lattice constant of La-doped sodium tantalate was larger than the other two using Rietveld analysis. The bonding state of the atoms and the ionic radius of La were larger than that of Sm, which increased the amount of strain and affected the lattice constant.

Keywords: Photocatalysis, Hydrothermal synthesis, Rare earth elements, Atomic bonding, Ionic radius

Email: saiki@sus.u-toyama.ac.jp

P33-Effect of alloying elements on the microstructure and properties of SnAgCu based lead-free solder alloys

T. Y. Li[1], S. T. Yu[1], Z. Dong[1*], J. Zhang[1]

[1]*Materials Genome Insititute,Shanghai University,200444, People's Republic of China*

Due to the harmful effect on human and environment, lead-bearing solder alloys have been banned in many countries. Developing the lead-free solders is essential to the rapid development of the modern electronic industries. Among all the lead free solders developed, SnAgCu (SAC) solder alloy is one of the most promising lead-free solders and has already been used in the electronic industry. However, the properties of SAC alloys still need to be improved to meet the higher demand from the modern electric industry. In the current study, a variety of alloying elements were introduced into SAC based solder alloys, and their effects on the microstructure and properties of solder alloys were evaluated. The results show that adding proper amounts of Bi and In into SAC solder alloys could improve both the strength and ductility. Meanwhile, the shear strength of the BGA joints could also be improved. Further adding amounts of Ni into the Bi, In-containing SAC solder alloy could improve the shear strength even higher. The current study provides the guidance for developing novel SAC-based solder alloys with optimized properties.

Keywords: Lead-free solder; SAC; Alloying.

Email: * zqdong@shu.edu.cn

P34-Microstructure observation of Al-1.0mass%Mg_2Ge-(0.4mass%Si) alloys aged at 473K

S. Murakata[1], T. Tsuchiya[2], S. Lee[2], S. Ikeno[3], and K. Matsuda[2, †]

[1]Graduate School of Science and Engineering, University of Toyama, Toyama, Toyama, 930-8555, Japan

[2] Faculty of Sustainable Design, Department of Materials Design and Engineering, University of Toyama , Toyama, Toyama, 930-8555, Japan

[3]Professor emeritus, University of Toyama, Toyama, Japan

It is known that a substitution for Si to Ge in Al-Mg-Si alloy can improve its mechanical property by aging heat treatment at relatively high temperatures. Precipitation sequence in Al-Mg-Ge alloy is suggested S.S.S.S → cluster → G. P. zone → Random type → parallelogram type, β" → β', A type → β. It is known that the Al-Mg-Ge alloy shows a higher maximum hardness as compared with the Al-Mg-Si alloy with aging treatment. And the maximum hardness of the Al-Mg-Ge alloy with Si addition also shows a higher hardness than that of without Si addition. In this study, the effect of Si addition on aging behavior in Al-Mg-Ge alloys was investigated with hardness measurement and Transmission Electron Microscope (TEM) observation. The chemical compositions of the alloys are Al-0.40Mg-0.61Ge (mass %) alloy (base alloy) and Al-0.44Mg-0.51Ge-0.40Si (mass %) alloy (Si added alloy). Both alloy homogenization treatment at 673K for 21.6ks after casting. Both samples with the thickness of 1mm and 0.2 mm were prepared by hot-and cold-rolling, followed by the solution treatment at 873K for 3.6ks and then quenched into chilled water. Afterwards, they were added at 473K. Vickers microhardness measurement was conducted by using Mitutoyo HM-101. TEM observation was conducted by using Topcon, EM-002B with accelerated voltage of 120 kV. There was no difference in hardness values at as. Q between the two alloys. And, Si added alloy shows a higher maximum hardness as compared with the base alloy. Furthermore, Si added alloy shows a shorter time to reach maximum hardness than base alloys. In TEM observation, precipitate cross section and those aspects were observed in both alloys. The number density of precipitates from precipitate cross section in the Si added alloy at the initial stage and peak hardness condition was increased compared to base alloy.

Keywords: Al-Mg-Ge, Precipitation, TEM

Email: †ikenolab@sus.u-toyama.ac.jp

P35-Long-range ferromagnetic ordering and novel phase transitions in macroscopic artificial kagome particle ice

J. J. Zhang[3], J. Y. Ge[3]

[1]*State Key Laboratory of Surface Physics, Department of Physics, and Laboratory of Advanced Materials, Fudan University, Shanghai 200433, People's Republic of China*

[2]*Collaborative Innovation Center of Advanced Microstructures, Nanjing, 210093, China*

[3]*Materials Genome Institute, Shanghai University, Shanghai 200444, People's Republic of China*

[4]*UVSOR Synchrotron Facility, Institute for Molecular Science, National Institutes of Natural Science, Myodaiji, Okazaki 444-8585, Japan*

[5]*UVSOR Synchrotron Facility, Institute for Molecular Science, Myodaiji, Okazaki 444-8585, Japan*

A totally new platform to study particle ice is proposed and realized. Easily manipulate each interaction unit. Directly see the ice state. Rich ways to manipulate the interaction, such as the magnet diameter, length et al. Everyone can do such experiment even in you office, at home, which will definitely attract much interest. For the first time, ferromagnetic ground state is realized experimentally in particle ice system. With our design, we are even able to reach an ultrastrong interaction region, where the long-range ordered FM state is broken down. For the first time, a new phase transition from FM1 state to FM2 state is observed. Such a state was even not predicted by theory.

Keywords: Ferromagnetic ground state, Novel phase, Manipulation

Email: 1693000514@qq.com

P36-TEM observation of Mg-2.2Zn-0.2In alloy aged at 473K

J. Ezura[1], T. Tsuchiya[2], S. Lee[2], S. Ikeno[3], and K. Matsuda[2, †]

[1]Graduate School of Science and Engineering, University of Toyama, Toyama, Toyama, 930-8555, Japan

[2] Faculty of Sustainable Design, Department of Materials Design and Engineering, University of Toyama , Toyama, Toyama, 930-8555, Japan

[3]Professor emeritus, University of Toyama, Toyama, Japan

Mg-Zn alloys are known as aged-hardened Mg alloy. The aging precipitation sequence is S. S. S. S. → G. P. zone → β_1'(rod-shaped precipitates perpendicular to the {0001}Mg plane), β_2'(coarse plate precipitates parallel to the {0001}Mg plane) → β and it is considered that the intermediate phase β_1' mainly contributes to the hardness. However, the age-hardenability of Mg-Zn alloy is relatively low. In recent years, attempts have been made to further improve the age- hardenability by adding a trace amount of an alloying element to Mg-Zn alloy. When the BOP value was calculated by the Dv-xα method for the selection of candidate additive elements, in showed a relatively high value. However, the age hardening behavior of Mg-Zn-In alloys has not been clarified.

In this study, the microstructure was observed using a transmission electron microscope with the aim of clarifying the effect of In addition on the aging hardening behavior of Mg-Zn alloys. This alloy was prepared by gravity casting. Homogenization was carried out at 603 K for 43.2 ks and the sample was hot rolled to 1 mm thickness. The solution treatment was performed at 603 K, 3.6 ks in an argon atmosphere , then quenched into water at 293 K. Aging treatment was conducted at 473K. TEM specimens were prepared by twin jet electrolytic polishing method using a solution of nitric acid : acetic acid : ethanol = 1.5 : 1.5 : 7 cooled to 263 K. Microstructure observation was carried out using transmission electron microscope (TEM, TOPCON EM-002B) under accelerated voltage of 120kV.

Keywords: TEM, Mg-Zn-In alloy, Precipitation, Aging

Email: †ikenolab@sus.u-toyama.ac.jp

P37-Reveal of free radicals in manganese-based catalysts and their roles during selective catalytic reduction of nitrogen oxide

L. M. Hou[1], Y. L. Wen[2], J. Z. Wu[1], Y. Yang[1], J. Zhang[2*], J. C. Zhang[1*], G. R. Qian[1]

[1]*Materials Genome Institute, Shanghai University, 333 Nanchen Road, Shanghai 200444, China*

[2]*SHU Center of Green Urban Mining & Industry Ecology, School of Environmental and Chemical Engineering, Shanghai University, No. 381 Nanchen Road, Shanghai 200444, China*

Manganese-based catalysts attract extensive attentions in low-temperature selective catalytic reduction (SCR) of nitrogen oxide (NO_x). However, seldom work focuses on the existence of free radicals and their roles in SCR. In this work, experiment and density functional theory are combined to reveal surface characterizations of manganese oxide and Ce/La-doped manganese oxides. As a result, superoxide radical (O_2^*) exists on manganese-oxide surface, produces nitrogen containing free radical, and functions as electron transfer between NO_x and NH_3 at 100 °C resulting in good NO_x conversion as well as N_2 selectivity at the same time. The O_2^* is born of accepting electrons on adsorbed oxygen through overlapped orbits of Mn-d and O-p. Additional metal doping increases the percentage of O_2^* among all oxygen species from 2.9 % to 6.9 % (Ce doping) and 5.1 % (La doping). The order of O_2^* percentage is consistent with the NO_x-conversion order at 100 °C , Ce doping (91.6 %) > La doping (55.7 %) > catalyst without doping (27.5 %). Above result helps to understand interface behaviors of manganese-based catalyst in SCR. This work is also in favor of developing more effective low-temperature catalysts.

Keywords: Selective catalytic reduction, Nitrogen oxide, Manganese oxide, Superoxide radical

Email: houlm8@163.com

P38-Synthesis of micro sized hollow Ceria particles prepared by spray dry pyrolysis

T. Hashizume‡, A. Saiki

Faculty of Sustainable Design, Academic Assembly, University of Toyama, Gofuku3190, Toyama,930-8555, Japan

The morphology of ceria microparticles prepared by a combination of spray drying and pyrolysis methods using cerium acetate and cerium nitrate hydrate as precursors was observed by scanning electron microscopy. It was observed that the sprayed nitrate solution was dried in a cyclone vortex flow to shape the particles, which were then directly subjected to pyrolysis reaction, resulting in oxide particles. The particles were found to be correlated with spray pressure, precursor solution concentration and particle size. The obtained particles were 3-16 micrometers in diameter.

Keywords: Spray pyrolysis, Cerium oxide, Micro sized hollow particle, Morphology

Email: ‡ hasizume@sus.u-toyama.ac.jp

ICPMAT 2022 Shanghai 中国
16th International Conference on the Physical Properties and Application of Advanced Materials
21st-23rd November, 2022

P39-Effect of Mo on Pitting Corrosion Resistance of Martensitic Stainless Steels

D. Nakato[1], K. Nagae[1], M. Hatakeyama[2] and S. Sunada[2]

[1]Graduate School of Material Science and Engineering for Education, University of Toyama, Gohuku Toyama, 930-8555, JAPAN

[2]Graduate School Material of Science and Engineering for Research, University of Toyama, 3190 Gohuku Toyama, 930-8555, JAPAN

The effect of Mo on the pitting corrosion resistance of martensitic stainless steels is investigated in this study. To evaluate pitting corrosion resistance, electrochemical experiments were conducted on samples with different Mo contents. The pitting potential (E_{pit}) increased with increasing Mo content, and the pitting corrosion resistance improved. The pitting current density (I_{pit}) was best suppressed at 1.75 mass%Mo, and the protection of the passive film was improved. However, at 2.50 mass%Mo, the highest Mo content, I_{pit} increased more than 20 times, and the protective property of the passive film was lost. The corrosion state was evaluated by observing the sample surface and cross section before and after corrosion. The δ-ferrite phase was precipitated at 2.50 mass%Mo. Preferential dissolution of the specimen was observed around the δ-ferrite phase.

Keywords: Corrosion, Stainless steel, Molybdenum

Email: m22c1615@ems.u-toyama.ac.jp

P40-Effect of Cu content on electrochemical activity in Mg-Cu binary alloys prepared by single role rapid solidification method

Y. Yamada[1], S. Fukui[2], Y. Fukuta[2], T. Tsukeda[2], T. Aida[2], H. Tabata[3], H. Kurihara[4], M. Suzuki[5]

[1]*Graduate school of science and engineering education, University of Toyama, Toyama, 930-8555, Japan*

[2]*Faculty of Sustainable Design, University of Toyama, Toyama, 930-8555, Japan*

[3]*Advanced Technology Laboratory. Chuetu Metal Works Co., Ltd., Toyama, 930-0298, Japan*

[4]*N/A, Saitama Industrial Technology Center (SAITEC), Saitama, 333-0844, Japan*

[5]*Faculty of Engineering, Toyama Prefectural University, Toyama, 930-0398, Japan*

Magnesium rechargeable batteries are expected to be the next-generation rechargeable ones due to their resource abundance, safe granular precipitation form, and high volumetric energy density compared with lithium-ion batteries. However, the reason why magnesium rechargeable batteries have not yet been put into practical use is that the overvoltage of the metal anode reaction is large and the reversibility is poor. Therefore, we are investigating the effects of various additive elements with the aim of developing anode materials for magnesium rechargeable batteries with better electrochemical activity. On the other hand, in ordinary magnesium alloys, transition metal elements such as Fe, Ni, and Cu are restricted to low concentrations as impurity elements that degrade corrosion resistance. Kurihara reported that in rolled Mg-Cu binary alloys, the amount of Mg 2 Cu increases with increasing Cu addition as well as the electrochemical activity. However, Cu content of 10% or more makes it difficult to be rolled. Therefore, our joint research team prepared Mg-Cu binary alloys ribbons with Cu contents exceeding 10% by using a single roll liquid rapid solidification method, which does not require a plastic forming process such as rolling, and investigated the electrochemical activity of each ribbon. The effect of Cu addition on electrochemical activity was discussed in terms of ribbon soundness, surface properties, crystal structure, and microstructure. Among the fabricated specimens, when the Cu content exceeded 15%, the brittleness of the ribbons increased and the specimens became unsound. In each alloy system, Mg-1%Cu and Mg-5%Cu showed the best discharge and charge reactivity.

Keywords: Magnesium rechargeable battery, Effect of chemical composition, Mg-Cud binary alloys

Email: ymd540812@gmail.com

P41-High-throughout synthesis of $La_{1-x}Sr_xTiO_3$ thin film and its characterizations

Y. Z. Wang[1], J. Han[1], H. F. Zhang[1], R. H. Ma[1], F. Chen[1*]

[1]*Materials Genome Institute, Shanghai University, Shanghai 200444, China*

As the typical perovskite materials, $LaTiO_3$ is a Mott insulator and $SrTiO_3$ is a band insulator. The crystal structure of $La_{1-x}Sr_xTiO_3$ exhibits orthorhombic *Pbnm* to orthorhombic *Ibmm* transition at x = 0.3 and then turns to the cubic *Pm3m* structure at x = 0.8. $La_{1-x}Sr_xTiO_3$ film undergoes a superconducting transition at a critical temperature $T_c \approx 300$ mK. Here we have synthesized all components of $La_{1-x}Sr_xTiO_3$ thin film with high-throughout method. $La_{1-x}Sr_xTiO_3$ thin film has been grown on the (00*l*) Si substrates by pulsed laser deposition, using the $SrTiO_3$ and $LaTiO_3$ polycrystalline targets. The optimal process parameters for growing continuous component $La_{1-x}Sr_xTiO_3$ thin film are determined. The component gradients of La and Sr are achieved by shifting the mask plate located between the substrate and the target. The X-ray diffraction and energy dispersive spectrum results showed that $La_{1-x}Sr_xTiO_3$ film was successfully obtained. The electric transport properties of $La_{1-x}Sr_xTiO_3$ were investigated using physical property measurement system.

Keywords: $La_{1-x}Sr_xTiO_3$ film, Pulsed laser deposition, Perovskite, High-throughout

Email: *chf001@t.shu.edu.cn

P42-Effect of microstructure on hardness of Mg-Sc-Zr alloys with α + β dual phase

H. Minami[1], T. Yamaguchi[2], T. Tsukeda[2], T. Aida[2], and H. Tabata[3]

[1]*University of Toyama, Graduate School of Science and Engineering, Toyama, 930-8555, Japan*

[2]*University of Toyama, Faculty of Sustainable Design, Toyama, 930-8555, Japan*

[3]*Chuetsu Metal Works Co., Ltd., Advanced Technology Laboratory, Toyama, 930-0298, Japan*

Magnesium has an hcp structure, however the addition of Li or Sc results in a composition range where the bcc structure is mixed. In particular, Mg-Sc alloys can be heat-treated to a single-phase bcc (β-phase) or hcp (α-phase) + bcc duplex structure to achieve high strength. It was also found to exhibit shape memory and superelasticity effects, which had not been reported among Mg alloys. However, Sc is currently expensive, and there are still few studies investigating the effects of adding a third element to Mg-Sc alloys or studies in which ductility was significantly improved.

In this study, we investigated the manufacturing process and addition of third element alloys with the aim of reducing manufacturing costs and improving mechanical properties for the practical use of Mg-Sc alloys. In the manufacturing process, the single-roll rapid solidification method was selected to reduce costs and the number of processing steps such as rolling. Balk material was also prepared to confirm whether the strength of the ribbons produced by the single roll rapid solidification method was sufficient. Zr was added as the third element in anticipation of microstructural refinement. If Zr can be added to Mg-Sc alloys without compromising their material properties, it is expected that the amount of Sc added to Mg alloy can be reduced.

Mg-20at%Sc alloy and Mg-10.3at%Zr alloy were used as master alloys for the fabrication of ribbon and balk materials, and weighed to obtain the target compositions. The target compositions were Mg-20at%Sc, Mg-19.6at%Sc-0.2at%Zr, and Mg-19.2at%Sc-0.4at%Zr, which are expected to undergo β single-phase treatment after Mg-Sc-Zr state diagram was created by Thermo-Calc.

The liquid rapid solidification equipment was fabricated by using an oxygen-free copper cooling roll without cooling water, inserting the weighed mother alloy into a crucible with a nozzle made of SUS430, melting it by induction heating, and injecting it with Ar gas onto a high-speed rotating roll. The production conditions were Ar atmosphere, injection pressure of 0.05 MPa, distance between nozzle and cooling roll 1.6 mm, and peripheral speed of cooling roll 30 m/s. Balk material was prepared by induction heating in a quartz glass crucible. Hardness was selected as a mechanical property, and Knoop hardness with shallow indentation was used to measure the hardness of ribbon, and Vickers hardness was used to measure the hardness of balk material, respectively. The effect of microstructure on hardness was also investigated. The surface microstructure of the ribbon was observed using FE-SEM. The cell size was calculated by the quadrature method using a microstructure photograph of the free-solidification surface of each ribbon. After each ribbon was embedded with room temperature hardening resin, microstructural observation of the cross-section was performed by low-vacuum SEM, and elemental analysis was

performed by EDS. Microstructural observations of balk material were made by low-vacuum SEM and FE-SEM. The crystalline phases were identified by XRD, and the peak intensities of the (110) diffraction peak for the bcc phase and the (10-11) diffraction peak for the hcp phase (bcc/hcp) were compared by subtracting the background values. Heat treatment was also performed to clarify the effect of Zr addition on the phase transformation behavior of the Mg-Sc alloy.

Keywords: Mg-Sc-Zr alloy, Hcp + bcc duplex structure, Microstructure, Hardness

Email: tubbc.32516.srconn@gmail.com